

UNCLASSIFIED
AD 433240

DEFENSE DOCUMENTATION CENTER
FOR
SCIENTIFIC AND TECHNICAL INFORMATION
CAMERON STATION, ALEXANDRIA, VIRGINIA



UNCLASSIFIED

NOTICE: When government or other drawings, specifications or other data are used for any purpose other than in connection with a definitely related government procurement operation, the U. S. Government thereby incurs no responsibility, nor any obligation whatsoever; and the fact that the Government may have formulated, furnished, or in any way supplied the said drawings, specifications, or other data is not to be regarded by implication or otherwise as in any manner licensing the holder or any other person or corporation, or conveying any rights or permission to manufacture, use or sell any patented invention that may in any way be related thereto.

RTD
TDR
67-3102

EXPERIMENTAL FRACTURE STUDIES AND
EQUATION-OF-STATE MEASUREMENTS

TECHNICAL DOCUMENTARY REPORT NO. RTD-TDR-67-3102

March 1968



Research and Technology Division
AIR FORCE WEAPONS LABORATORY
Air Force Systems Command
Kirtland Air Force Base
New Mexico

This research has been funded by the
Defense Atomic Support Agency under WEB No. 15,024

Project No. 5776, Task No. 577601

(Prepared under Contract AF 29(601)-5382 by N. A. Louie,
W. H. Andersen, and M. H. Wagner, Aerojet-General
Corporation, Downey, California)

433240

**Research and Technology Division
Air Force Systems Command
AIR FORCE WEAPONS LABORATORY
Kirtland Air Force Base
New Mexico**

When Government drawings, specifications, or other data are used for any purpose other than in connection with a definitely related Government procurement operation, the United States Government thereby incurs no responsibility nor any obligation whatsoever; and the fact that the Government may have formulated, furnished, or in any way supplied the said drawings, specifications, or other data, is not to be regarded by implication or otherwise as in any manner licensing the holder or any other person or corporation, or conveying any rights or permission to manufacture, use, or sell any patented invention that may in any way be related thereto.

This report is made available for study upon the understanding that the Government's proprietary interests in and relating thereto shall not be impaired. In case of apparent conflict between the Government's proprietary interests and those of others, notify the Staff Judge Advocate, Air Force Systems Command, Andrews AF Base, Washington 25, DC.

This report is published for the exchange and stimulation of ideas; it does not necessarily express the intent or policy of any higher headquarters.

Qualified requesters may obtain copies of this report from DDC. Orders will be expedited if placed through the librarian or other staff member designated to request and receive documents from DDC.

RTD TDR-63-3102

FOREWORD

This document, the final report under Contract AF 29(601)-5382, is submitted to the Air Force Weapons Laboratory, Kirtland Air Force Base, New Mexico. The work was performed during the period June 1962 to October 1963.

RTD TDR-63-3102

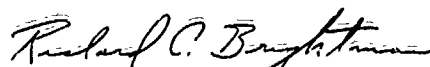
ABSTRACT

Studies of crack-propagation rates in plastics and polycrystalline aluminum were conducted to help test the validity of Waldorf's fracture theory. Results of these studies revealed that the omission of plastic-flow effects in the Waldorf equation is a serious neglect, since this flow can appreciably alter the effective stress at the crack tips under suitable conditions. This phenomenon will modify the temperature dependence of the strength of the material from that given by the theory and its a-priori determined parameters. A discussion of fracture-time delay is also included.

Dynamic-compression data were experimentally determined for four re-entry vehicle materials: Avcoat II, Chopped Nylon Phenolic, RAD 60, and Series 124A Resin. These data have been used to formulate a Hugoniot equation of state for each material.

PUBLICATION REVIEW

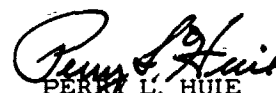
This report has been reviewed and is approved.



RICHARD C. BRIGHTMAN
Lieutenant USAF
Project Officer



JOHN J. NEUER
Colonel USAF
Chief, Physics Branch



PERRY L. HUIE
Colonel USAF
Chief, Research Division

CONTENTS

	Page
1. INTRODUCTION	1
2. SUMMARY	1
a. Time Delay of Fracture	1
b. Equation-of-State Measurements	3
3. TIME DELAY OF FRACTURE.	4
a. Crack-Propagation Studies	4
b. Time-Delay Studies	18
4. EQUATION-OF-STATE MEASUREMENTS	25
a. Determination of Shock-Wave Velocity	25
b. Gas-Gun Experiments	37
c. Explosive-Flying-Plate Experiments	37
d. Experimental Results	40
References	52
Distribution	55

ILLUSTRATIONS

Figure		Page
3-1.	Sample Preparation	8
3-2.	Tensile-Testing Apparatus	9
3-3.	Film Sequence of Crack Propagation in Epoxy Sample at 100° C.	11
3-4.	Stress vs Time (Epoxy Sample at 100° C)	12
3-5.	Fractional Change of Crack Length vs Time (Epoxy Sample at 100° C.)	13
3-6.	Proposed Crack-Velocity Experiment	15
3-7.	Wave Diagram for Plate Impact (Hydrodynamic Model)	20
3-8.	Wave Diagram for Plate Impact (Elastic-Plastic Model)	21
3-9.	Davies Bar	23
3-10.	Photostress Experiment	24
4-1.	Transducer Polarity Tester	27
4-2.	Transducer Placement	28
4-3.	Transducer Jig	29
4-4.	Target With Transducer Assembly	30
4-5.	Test Circuit	31
4-6.	Typical Film Record	33
4-7.	Gas Gun	38

II ILLUSTRATIONS

Figure		Page
4-8.	Triggering and Timing-Pulse Circuit for Gas-Gun Tests	39
4-9.	Triggering and Timing-Pulse Circuit for Explosive Tests	43
4-10.	Shock Velocity vs Particle Velocity (Avcoat II)	44
4-11.	Dynamic-Compression Curve (Avcoat II)	45
4-12.	Shock Velocity vs Particle Velocity (Chopped Nylon Phenolic)	46
4-13.	Dynamic-Compression Curve (Chopped Nylon Phenolic)	47
4-14.	Shock Velocity vs Particle Velocity (RAD 60)	48
4-15.	Dynamic-Compression Curve (RAD 60)	49
4-16.	Shock Velocity vs Particle Velocity (Series 124A Resin)	50
4-17.	Dynamic-Compression Curve (Series 124A Resin)	51

1. INTRODUCTION

This final report discusses work performed by Aerojet-General Corporation under Contract AF29(601)-5382. The program objectives were as follows:

- a. To determine the shock-stress/time-delay relation and the form of the associated crack-propagation velocity for fracture in homogeneous and/or single-crystal materials.
- b. To determine Hugoniot equations of state for four selected solid materials.

A summary of work in the preceding areas is presented in Section 2. Section 3 discusses the fracture studies; Section 4, the equation-of-state determinations.

2. SUMMARY

a. TIME DELAY OF FRACTURE

Experimental studies were conducted to help test the validity of a theory, developed earlier by Waldorf, that attempted to explain the delay which exists between the time of applying a tensile stress to a material and the time of material fracture.

The experimental work primarily comprised investigations of crack-propagation rates, since Waldorf's theory predicts that a stress-dependent crack velocity is the controlling factor in the fracture time of polycrystalline or heterogeneous materials. Experiments were conducted by subjecting a sample material with a small surface crack to a simple tensile force, which was applied perpendicular to the line of the crack by an Instron tensile tester. The crack velocity and the applied stress were then measured as a function of time. Also briefly considered was the influence of ambient temperature. Materials used in the studies were Plexiglas, an epoxy resin, and polycrystalline aluminum. These investigations were intended to test both the form of the Waldorf equation under moderate stress conditions, and the values of the various parameters used in the equation.

Preliminary studies were conducted on the fracture-delay time of a material under shock loading, this work primarily concerned developing techniques by which meaningful experimental fracture-delay times could be measured under shock loading. An evaluation was also made of the Waldorf equation with regard to published studies related to crack propagation.

Results of Crack-Propagation Studies

The cracks were generally found to widen slowly under tension without increasing in length, and then to suddenly undergo a very rapid increase in length. This phenomenon made it difficult to measure the crack velocity and to accurately correlate the tensile stress with the velocity. The crack velocity is clearly a nonlinear function of the tensile stress, but the results were not sufficiently accurate or reproducible to definitely show that the relationship is exponential. It is possible, for wide ranges of tensile stress, that a hyperbolic sine function may be a more useful expression.

Photographs obtained of the crack propagation, showing considerable plastic flow at the crack tips, and observations made of the initial crack widening before propagation indicate that a serious omission exists in the Waldorf equation, i. e., the omission of plastic-flow effects. These effects can alter the effective stress at the crack tips from that calculated from the applied tensile stress, giving a different temperature dependence for the strength of the material than would be calculated from the Waldorf equation (this may possibly explain the recent observations at Boeing that the spall threshold for Plexiglas is greater at higher temperatures). The preceding also explains the magnitude of the activation energy found by Zhurkov for the fracture of aluminum. When the experimental surface energies of various plastics reported in the literature are related to the effective activation energy of the Waldorf equation, a similar conclusion may be made that plastic-flow effects are of importance in crack propagation. Finally, there are also examples in the literature showing that plastic flow can completely control the creep and fracture rates of certain materials under certain conditions, in which case crack propagation per se is of minor importance.

The inclusion of plastic flow in Waldorf's equation would tend to change the values of certain parameters therein. Thus, it appears that the Waldorf expression as written should be most useful and reliable for very brittle materials under nominal stress-loading

conditions in which plastic flow is of little importance. When plastic-flow effects are important, the preceding parameters cannot usually be evaluated a priori with any degree of confidence, even as to their order of magnitude.

Studies reported in the literature indicate that the limiting crack velocity used in Waldorf's equation, and the approach to this velocity under very high stress conditions, may not be completely valid.

Results of Short-Time-Delay Studies

Investigations were undertaken to perfect the proposed "null spallation method" of measuring the fracture-time delay of a material under shock loading. The studies were primarily concerned with determining the shock waveshape in the material, since the accuracy of the measured time delay depends on the accuracy of the assumed waveshape. Experimental studies of waveshape were conducted using a Davies bar method, a quartz transducer, and a photostress technique. None of these techniques was refined to a degree at which it could be used for obtaining accurate data.

b. EQUATION-OF-STATE MEASUREMENTS

Equations of state for four re-entry vehicle materials (Avcoat II, chopped nylon phenolic, RAD 60, and Series 124A resin) were experimentally determined using the deceleration or plate-impact method. The plates were projected by means of either a gas gun or an explosive configuration, depending on the desired shock pressure. Measurements obtained of the plate velocity prior to impact (using shorting-pin probes) and of the shock velocity (D) in the target (using piezoelectric transducers) enabled computations to be made of the dynamic-compression variables: pressure (P), compression ($\rho/\rho_0 = \eta$), and particle velocity (u). These data were used to compute a linear relation of shock velocity to particle velocity,

$$D = a u + b \text{ mm}/\mu\text{sec} \quad (2-1)$$

from which was derived an equation of state,

$$P = c \frac{(\eta - 1)\eta}{(d - \eta)^2} \text{ kbar} \quad (2-2)$$

The values of a, b, c, and d for the four materials are given in the following:

Material	a	b	c	d
Avcoat 1	1.66	2.02	103	2.52
Chopped Nylon Phenolic	1.18	2.95	3250	6.55
RAM 60	1.07	1.53	6210	15.30
Series 12-A Resin	1.40	2.40	439	3.50

3. TIME DELAY OF FRACTURE

Experimental evidence indicates that a time delay occurs prior to fracture when a tensile stress is applied to either plastics (Reference 1 and 2) or metals (Reference 3). This delay, which exponentially decreases with increasing stress, is also a function of the temperature, chemical composition, and physical properties of the material.

In an earlier investigation conducted by Aerojet, Waldorf (Reference 4) developed a theory of fracture that encompassed both homogeneous and polycrystalline materials. The terminal phase of the present program has been concerned with experimental studies that were performed to help test the validity of Waldorf's theory. Toward this end, studies have been conducted to help elucidate the mechanism of fracture both in homogeneous and heterogeneous materials, particularly with regard to elucidating the stress dependence of crack-propagation rates. Fracture-delay times at high (shock) stress levels have also been investigated.

a. CRACK-PROPAGATION STUDIES

Fracture of Homogeneous Materials

The rate of bond rupturing in a homogeneous material is assumed to be constant throughout the material, rather than being concentrated as observed in crack propagation. For a constant stress, σ_0 , Waldorf predicts a relationship to the fracture delay time, t_c , as

$$t_c = \frac{1}{\omega} \exp \left[(E_0 - \sigma_0 \delta_a / a \eta_0) / kT \right] \quad (3-1)$$

where

E_o = binding energy of the undisturbed material
(sublimation energy)

a = a numerical constant = $(e - 1)/e$

η_o = number of atoms per square centimeter of area
perpendicular to σ_o

δ_o = average distance between the centers of the mutually
bound atoms or molecules in the unstressed state

ω = the inverse of the time required for the atom or
molecule to traverse the distance δ_o at mean thermal
velocity

k = Boltzmann's constant

T = absolute temperature

It should be noted that relaxation processes associated with self-diffusion are not included in the derivation of Equation 3-1. However, Bueche (Reference 2) found that such processes are the controlling factor for the time-dependent fracture of plastics. When the relaxation processes were considered, Bueche obtained a relation with the same form as Equation 3-1, but eliminated the anomalous error in ω by employing different constants. Bueche assumed that relaxation times are much shorter than the fracture time, so that the net effect is a general weakening of the bond after self-diffusion is essentially complete.

For plastics above the glass temperature, the effect of self-diffusion may be such as to partially relieve the tensile stress; therefore, the relaxation time becomes a significant portion of the fracture time. The temperature dependence in Waldorf's formula is such as to decrease the fracture time for increasing temperature. With increasing temperature, however, the effect of self-diffusion is so enhanced that it may be possible (for certain materials under suitable conditions) that the fracture time would increase for some specific temperature rise under constant stress.

Fracture of Polycrystalline Materials

Waldorf assumed that the fracture of polycrystalline materials occurs through the propagation of small cracks or microcracks which grow under the influence of the applied stress until they join to form a continuous fracture surface spanning the material. The fracture mechanism apparently follows the boundaries of the crystalline grains. The fracture time for neighboring drops to coalesce, i.e., the fracture time for polycrystalline materials, is $t_{cp} = a/v$, where v is the crack velocity and a is one-half the mean tip-to-tip spacing of the cracks (or, alternatively, one-half of the crack length).

The crack-propagation velocity is given by $v = d_0/t_c$, where $d_0 = (1/4) \cdot (ac)^{1/2}$, and c is one-half of the crack thickness. The value of t_c is given by Equation 3-1, except that the effective stress, σ , at the crack tips is related to the applied stress, σ_0 , by

$$\sigma = \sigma_0 (1 + 2Q) \quad (3-2)$$

where $Q = (a/c)^{1/2}$. Hence,

$$t_{cp} = 4Q t_c \quad (3-3)$$

The crack velocity is given by

$$v = \frac{1}{4} (ac)^{1/2} \omega \exp \left[- (E_0 - \delta_0 \sigma_0 (1 + 2Q) / a \eta_0) / kT \right] \quad (3-4)$$

Regardless of the extent of the stress, cracks cannot propagate faster than the Rayleigh wave velocity, c_R , in a material. Waldorf accounted for this effect by the following empirical equations:

$$v = \frac{d_0}{t_c} (1 - v^2/c_R^2)^{1/2} \quad (3-5a)$$

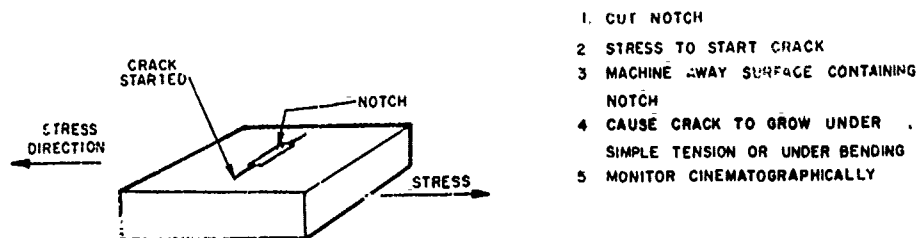
$$\sigma = \sigma_0 (1 + 2Q) (1 - v^2/c_R^2)^{-1/2} \quad (3-5b)$$

The same factors considered in the discussion of self-diffusion would apply to crack propagation, and, as Waldorf has indicated (but does not use), plastic-flow effects could have an important effect on the initiation of crack movement.

Experimental Work

Basically, the experiments were conducted by subjecting a sample material that had a small surface crack to a simple tensile force, which was applied perpendicular to the line of the crack. The samples were milled to a 4.0- x 1.0- x 0.5-in. rectangular body, and were prepared for testing by cutting a small notch in the center of the large face, perpendicular to the long axis. Each sample was then slowly stressed by flexure until a fine crack started to grow from the notch into and along the surface of the material. The notched face was then machined until only the fine crack remained, as shown in Figure 3-1.

The samples were tested in simple uniaxial tension on a Model TTC Instron Tensile Tester. This machine holds the samples by means of a constant and uniform moving crosshead; load measurements were made using sensitive load cells that registered the data on a recording oscillograph. To study the crack propagation, a Fastax camera (capable of 18,000 frames/sec) was fixed to photograph the sample perpendicular to the direction of strain. A pulse generator was connected between the camera and oscillograph for time correlation, as shown in Figure 3-2. The studies were initially conducted with Plexiglas; however, it was found that the fracture proceeded too rapidly for resolution by the experimental setup, and that the entire fracture process occurred sometime between frames on the film. More specifically, the crack was found to slowly widen under tension without increasing in length, then to suddenly undergo a very rapid increase in length. These observations agree with Irwin (Reference 5), who states that "the force-response relationship for crack extension in various materials shows that onset of rapid fracture usually occurs in a relatively abrupt manner," and that the time rate of the crack extension can be increased several orders of magnitude by a small change in tensile stress if the stress is close to the critical value.



1. CUT NOTCH
2. STRESS TO START CRACK
3. MACHINE AWAY SURFACE CONTAINING NOTCH
4. CAUSE CRACK TO GROW UNDER SIMPLE TENSION OR UNDER BENDING
5. MONITOR CINEMATOGRAPHICALLY

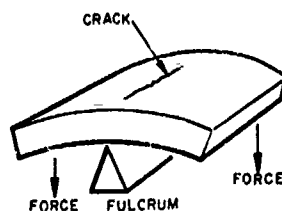
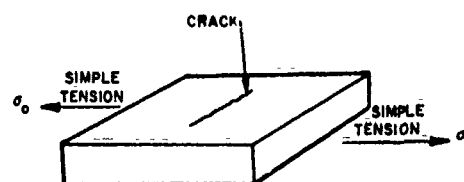
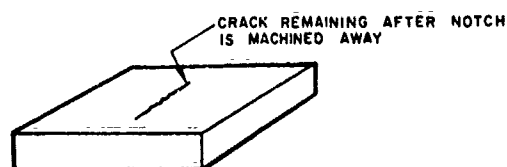


Figure 3-1. Sample Preparation.

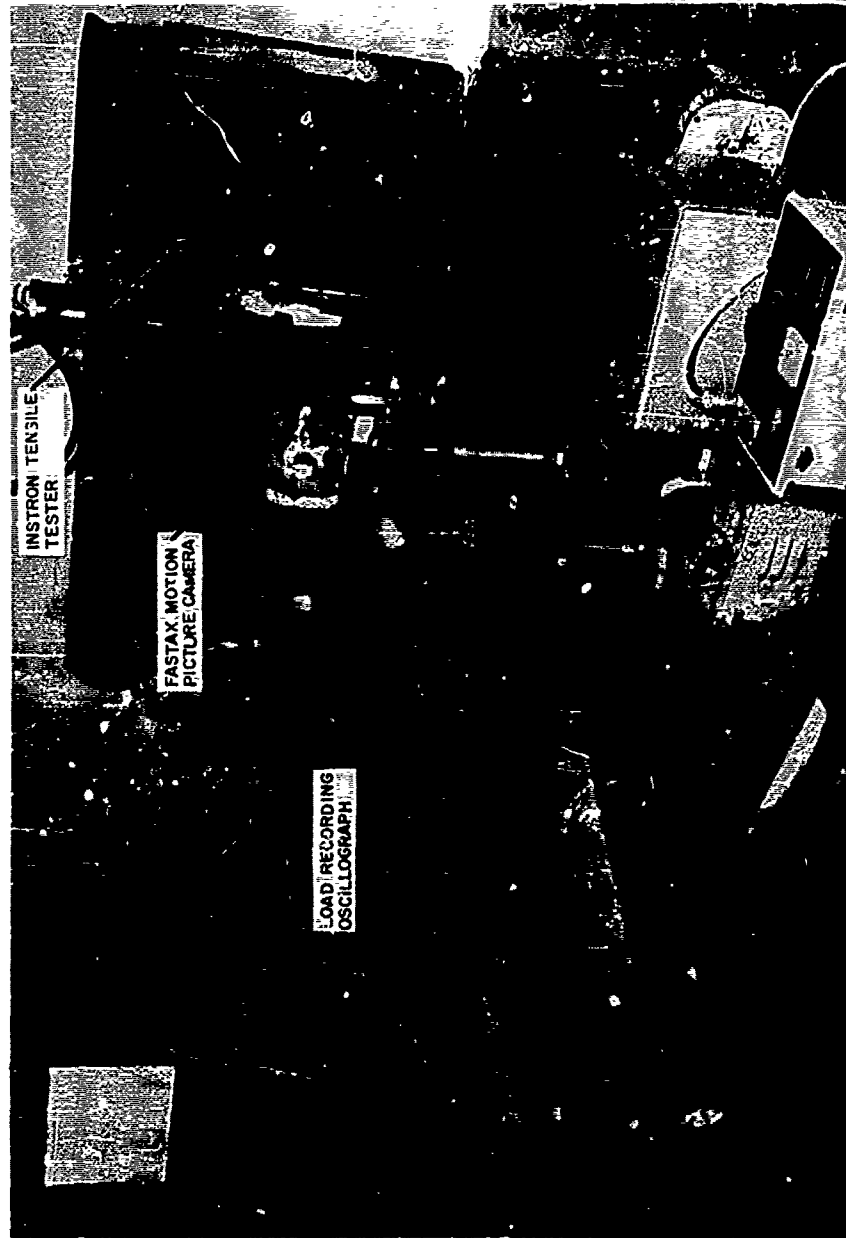


Figure 3-2. Tensile-Testing Apparatus.

Test samples were consequently fabricated from an epoxy resin, and although the preceding problem was still present, it was less pronounced; some photographs were obtained that clearly showed the growth of the crack to complete rupture of the specimen. A typical film sequence for a sample maintained at 100°C is given in Figure 3-3, and the variation of stress with time as measured by the load cells is shown in Figure 3-4. As shown in the illustrations, considerable plastic flow with attendant stress relief occurs prior to crack movement. In addition, the ratio of crack length to crack width changes considerably.

Figure 3-5 graphically depicts crack length as a function of time, showing the variation of crack velocity with crack length. By differentiating the curve in this illustration with respect to time, the velocity can be determined as a function of time; by correlating the resultant curve with the stress-time curve of Figure 3-4, estimates can be made of the stress dependence of the crack velocity.

Typical experimental data reduced in the preceding manner showed the crack velocity to be roughly an exponential function of the stress, as would be expected from the theory. In some cases, the relatively long portion of the curve before the rise can also be interpreted in terms of a hyperbolic sine function. Quite generally, the relationship is nonlinear over a large range of stress; however, the curvature was not reproducible, and hence definitive conclusions regarding the exact functional form of the crack velocity with stress could not be made.

It is believed that one principal source of the nonreproducibility is due to the plastic flow, which was clearly noticeable at the crack tips. This flow changes the stress magnitude so that the true stress at the crack tips is not the stress computed from the applied stress to the sample (clearly illustrating that the Waldorf equation is not adequate for materials or conditions in which plastic flow accompanies the crack propagation).

Fracture studies of the epoxy resin were conducted at initial temperatures of 80°F and at 0 and 100°C . Results of tests conducted at 80°F and 0°C exhibited the fracture behavior described in the preceding discussion; at 100°C , a fairly constant slow velocity was initially evidenced, followed by a short-duration high-velocity region to complete separation. It was not possible to obtain reproducible data, however, even using samples maintained at high temperatures and making various minor modifications of the technique.

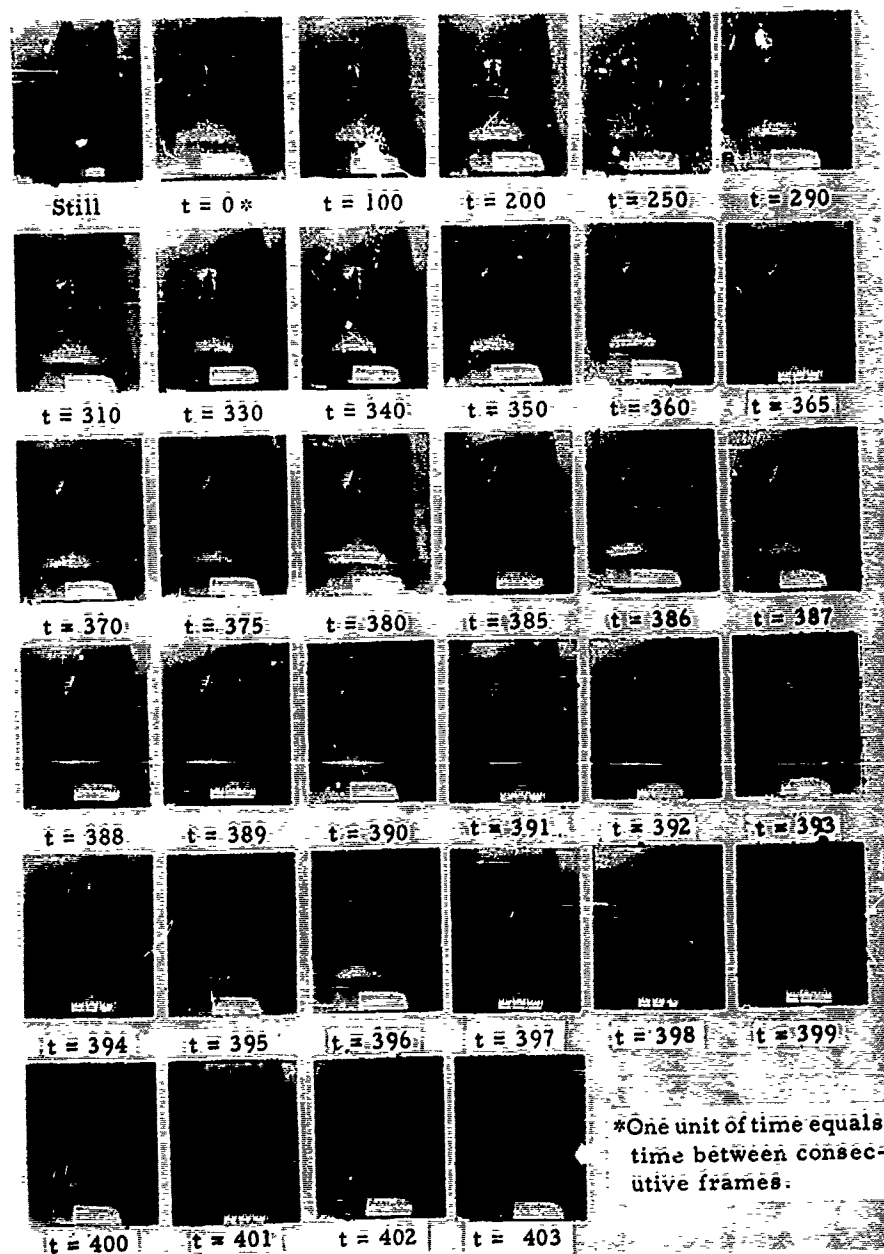


Figure 3-3. Film Sequence of Crack Propagation in Epoxy Sample at 100°C .

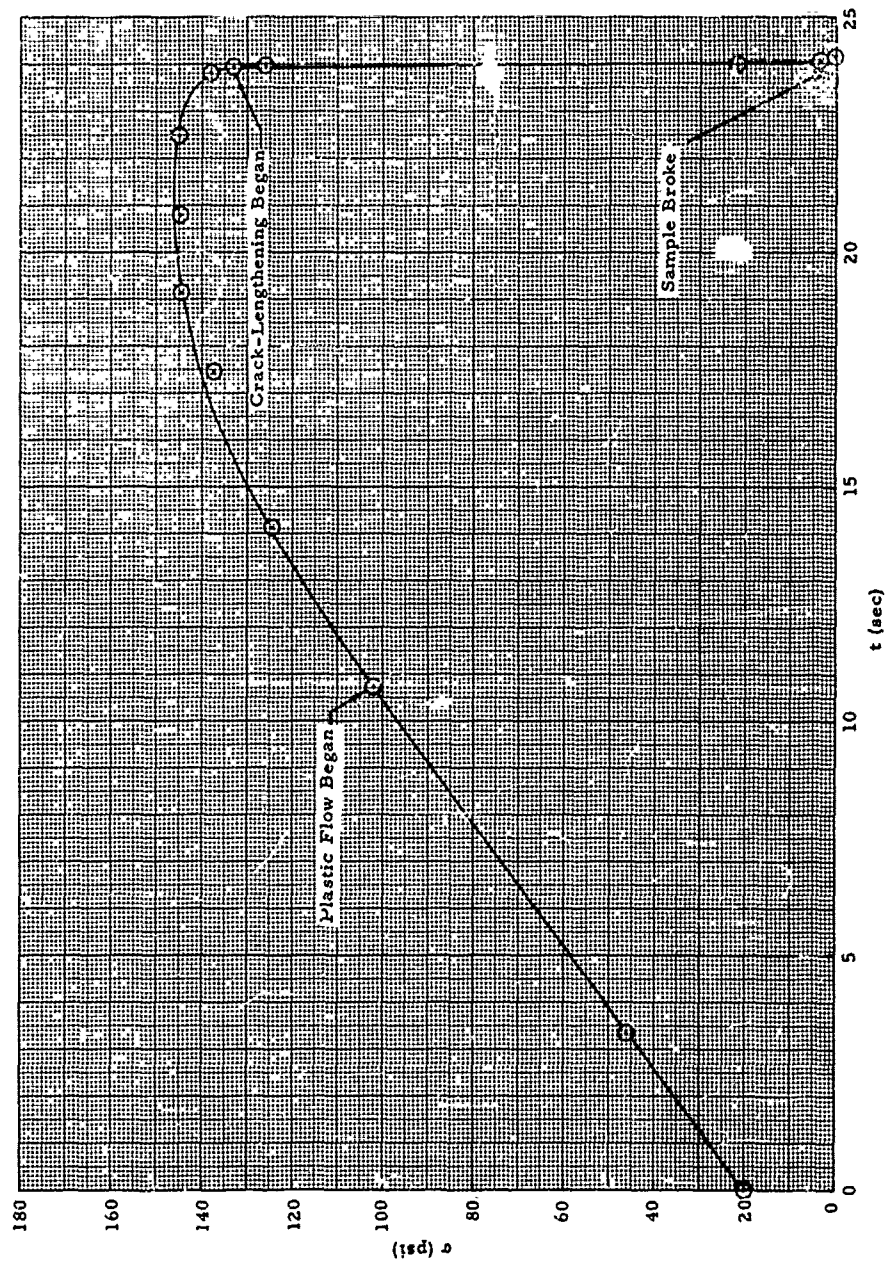


Figure 3-4. Stress vs Time (Epoxy Sample at 100°C).

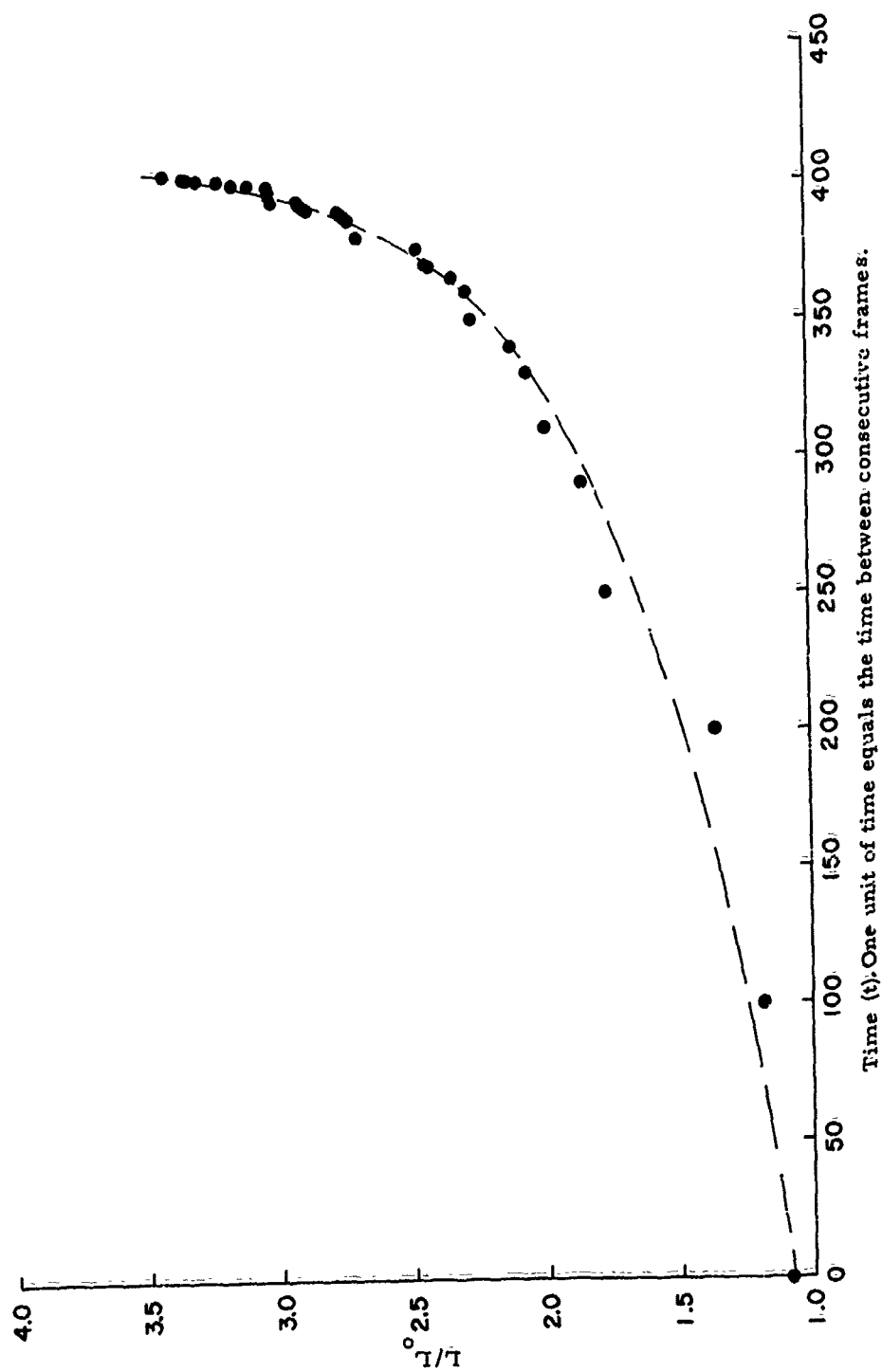


Figure 3-5. Fractional Change of Crack Length vs Time (Epoxy Sample at 100° C).

A part of the reproducibility problem appeared to be the difficulty of determining exactly where the crack tip was at any given time. Thus, even under microscopic examination, ordinary cracks extended further into the material than could be readily ascertained, since only the portion of the crack that was large enough to diffract light could be detected.

Another problem is presented in measuring the true stress applied, since it is difficult to accurately determine the change in area over which the force is applied as the crack grows (three dimensionally). It was also found that the time from initiation of the applied force to the beginning of crack growth varied so much that it was difficult to catch the event with the camera at high framing speeds (because of the short running time of about 1 sec).

In considering the preceding problems, it appears that it would have been more desirable to direct the original work to metals, rather than plastics, since metals undergo considerably less plastic flow; however, results of preliminary studies with polycrystalline aluminum also did not tend to give reproducible rate data.

An alternate experimental method has been formulated (Figure 3-6) that should allow successful measurements to be made of crack velocities in well-known materials, e.g., aluminum. In this technique, the measurement of the crack velocity would be made as the crack broke the thin metal strips, and triggering would be accomplished by breaking the strip closest to the initial crack tip. An estimate of the plastic flow prior to crack growth may be made by measuring the increase in resistivity of the trigger strip.

Another technique considered (but not developed) for measuring crack velocities would use polarized light and a photoelastic coating of known fringe constant on a thin sheet of the sample. Employing this method, the stress concentration at the crack tip and its position could be accurately determined.

Discussion

Although recent experimental studies did not allow a rigorous test of the Waldorf theory, results of the investigations indicated a serious flaw in the theory by omission of self-diffusion/plastic-flow effects. Under conditions in which the fracture is partially ductile, e.g., high temperatures, stresses, and purity of materials, the preceding effects will be important in such materials as aluminum, lead and pure iron, tin, and many plastics. It thus appears that the Waldorf

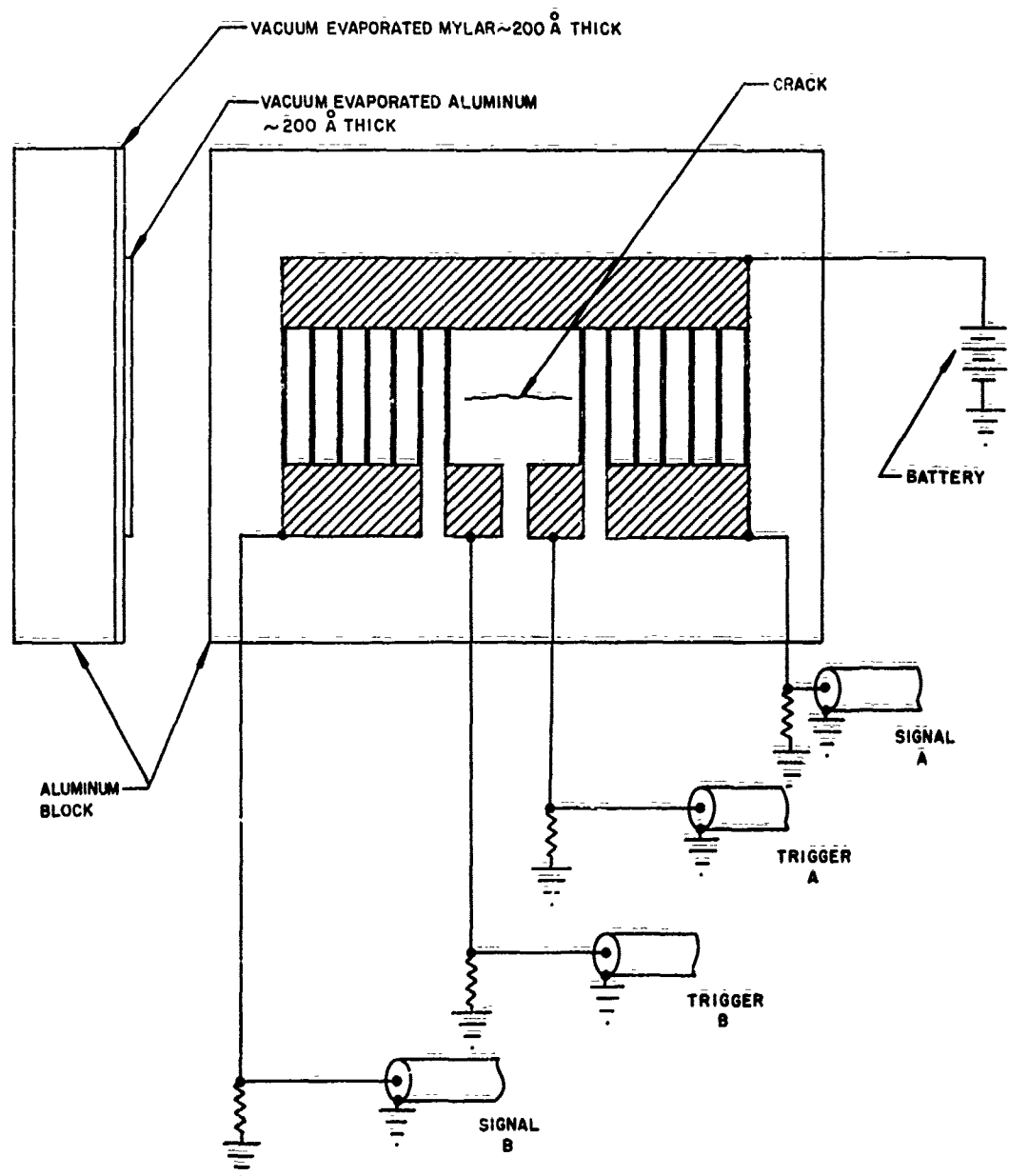


Figure 3-6. Proposed Crack-Velocity Experiment.

expression in its present form is most useful (and reliable) for materials undergoing brittle fracture, if theoretical values are to be used for its various parameters. However, if certain constants can be left arbitrary and evaluated from experimental fracture data, then there is reason to believe that the Waldorf theory is reasonably reliable for extrapolation purposes (but there are several fracture theories in the literature that will also fit the latter statement).

Andersen (Reference 6) has argued that a dual mechanism involving both sublimation (bond breaking) and self-diffusion (plastic flow) is required to explain the creep and fracture of various materials over a very wide range of temperature, stress, and composition. Depending on the conditions, it is thus possible that the creep or fracture rate can be controlled by either bond breaking, plastic flow, or both (simultaneously), as experimentally shown by plots of the logarithm of the creep or fracture rate vs the tensile stress for various ambient sample temperatures.

Bond breaking will give a linear temperature dependence of the rate (extrapolated to zero stress conditions), which gives a constant activation energy equal to the sublimation energy. Plastic flow gives the energy of self-diffusion, whereas both mechanisms simultaneously lead to intermediate values of the activation energy and the temperature dependence is not linear. Experimental samples of all of these behaviors are in the literature.

The other important case that must be considered is when the fracture is semibrittle in behavior and involves crack propagation, while plastic flow is simultaneously tending to reduce the effective stress at the crack tips. This condition should usually be of most importance when shock stress is involved, since the stress will be very high and the fast loading should give brittle fracture behavior. In this case, both mechanisms act simultaneously, but the temperature dependence of the rate will now be linear rather than nonlinear (as when the plastic flow was tending to produce voids rather than to reduce the stress at the crack tips).

The mechanism whereby plastic flow reduces the stress at the crack tips is believed to be responsible for the activation energy of 55 kcal/mole, which Zhurkov found for aluminum (Reference 3). The sublimation energy of aluminum is 75 kcal, whereas the energy for self-diffusion is 35 kcal. For the larger stresses, plastic flow lowers the effective stress at the crack tips below that which would be computed from the experimental stress, thus lowering the apparent

activation energy. For very low stresses, no plastic flow is involved. It has previously been shown (Reference 6), using Zhurkov's data, that the activation energy then increases as expected from 55 kcal to the sublimation energy.

Results of the most recent experimental studies, while not adequate to rigorously test the stress dependence of Waldorf's crack-velocity expression, do indicate that the velocity increased approximately exponentially with stress at low and moderate stresses (as predicted).

Irwin (Reference 5) states that after the onset of rapid crack extension, the velocity of the crack increases with an increase in the stress. However, for stress values of approximately 5 to 10 times the critical stress, there is relatively little further increase of crack velocity (as expected from Waldorf's theory, since a limiting crack velocity will be approached or reached). Irwin states that the velocity at high stresses appears to approach a limiting speed of about one-half of the shear-wave velocity. This value may be compared to the Rayleigh wave velocity, which was used as the limiting speed by Waldorf. Dulaney and Brace (Reference 7) give the limiting velocity as $(2\pi E/k\rho)^{1/2}$, where E is Young's modulus, ρ is the density of the material, and k is a constant whose value depends on the stress and displacement fields about the moving crack.

For a material with a Poisson ratio of 0.25 (typical metal), it was deduced that $(2\pi/k)^{1/2} = 0.38$, giving the limiting velocity as about 0.72 of the Rayleigh wave velocity (essentially consistent with the statements of Irwin). Dulaney and Brace theoretically deduced and experimentally found that the limiting velocity is approached in a hyperbolically asymptotic manner. This conclusion does not agree with the form proposed by Waldorf, i.e., Equation 3-5.

Irwin states that at very high tensile stresses, an increase in stress causes branching of the crack but no further increase in its velocity. This branching, i.e., the formation of subsidiary or parasitic cracks off the main crack at high stress levels, was also observed by Dulaney and Brace and by Benbow (Reference 8). Branching may arise from putting in energy faster than the running crack can absorb it, such as further increasing the stress when the velocity is near the limiting velocity, and from inhomogeneities in the material that may alter the stress distribution.

It should also be remembered that the stress distribution at the tip of a real crack (References 9 and 10) is considerably more complex than the simple expression used by Waldorf for a two-dimensional crack. However, it appears that the stress distribution employed by Waldorf is certainly adequate for use in present-day fracture-rate expressions.

Benbow (Reference 8), Berry (Reference 11), and others (see references in these papers) have experimentally determined the fracture surface energies, E_g , of various plastics. While rates of crack propagation or fracture were not studied per se, these investigations are directly related to rate studies in that the fracture surface energy is directly proportional to the effective activation energy (not the zero-stress activation energy) in the Waldorf expression, i. e.,

$$E_g = a' \left[E_0 - \delta_0 \sigma_0 (1 + 2Q)/a \eta_0 \right] \quad (3-6)$$

where a' denotes proportionality. Benbow found that the fracture surface energy of Perspex increases slightly with increases in the ambient temperature of the material. This effect indicates that the effective activation energy is a weak function of temperature.

The effective activation energy expression of Waldorf is not a function of temperature. However, in line with the previous discussions involving self-diffusion and plastic flow, an increase in temperature enhances the plastic flow, which will tend to lower the stress at the crack tips (tending to increase the effective activation energy). This explanation is also consistent with studies recently reported by Penning, Young, and Prindle (Reference 12), who found that the spall threshold is an increasing function of temperature for Plexiglas. The studies of Benbow and Berry show that the fracture surface energy of a material is a function of composition and physical condition (defects), a relationship to be expected on the basis of Waldorf's theory.

b. TIME-DELAY STUDIES

In any determination of stress/time-delay measurements, knowledge of the shock-wave profile is of paramount importance. Most of the time-delay experiments, e. g., the "null spallation method," assume the presence of a square wave; in general, however, such waves do not occur more than momentarily.

The usual method of approximating square waves is by impacting the test sample with a flying plate. As shown in Figure 3-7, according to hydrodynamic theory (Reference 13) when the driver and target are of the same material, a rarefaction fan originates at the rear free surface of the driver and ultimately degrades the shock front. While the intersection of the head of the rarefaction fan with the shock front does not occur for comparatively long distances for low enough pressures, the squareness of the tail of the shock is immediately affected. The situation is more complex at the free surface of the target, since the shock in the target is also reflected as a rarefaction fan, resulting in a trapezoidal wave rather than the square wave desired. While this combined effect can be minimized by using comparatively weak shocks, it may introduce a large uncertainty into the time-delay experiments where, as in the "null spallation method," small differences are significant.

There is evidence (Reference 14) that the structure of the shock induced into the target is even more complicated than the usual hydrodynamic theory would predict, and that an elastic rarefaction precedes the plastic rarefaction. After catching and attenuating the shock front, the elastic rarefaction reflects back and forth between the shock front and the plastic rarefaction (Figure 3-8). Although a model has been proposed to describe this premature attenuation in 2024 aluminum, it is not necessarily directly applicable to such materials as plastics. In any case, it would be extremely difficult (if possible at all) to accurately calculate the shock-pressure profile as a function of travel in these materials.

It was thus apparent that a method of accurately determining the pressure profile around the time of fracture was necessary before the actual stress/time-delay experiments could be performed. As initially planned, these preliminary experiments were to be conducted using the rotating impact machine, which was completed and installed during the second quarterly period of the program; however, the attainable impact planarity of the rotary impact machine was found to be inadequate. During the fourth quarterly period, a low-velocity gas gun was made available with which adequate planarity could be achieved, but it was necessary to employ this device almost exclusively in determining the low-pressure dynamic compression points for three of the re-entry materials. Therefore, the proposed experiments progressed just slightly beyond the conceptual stage.

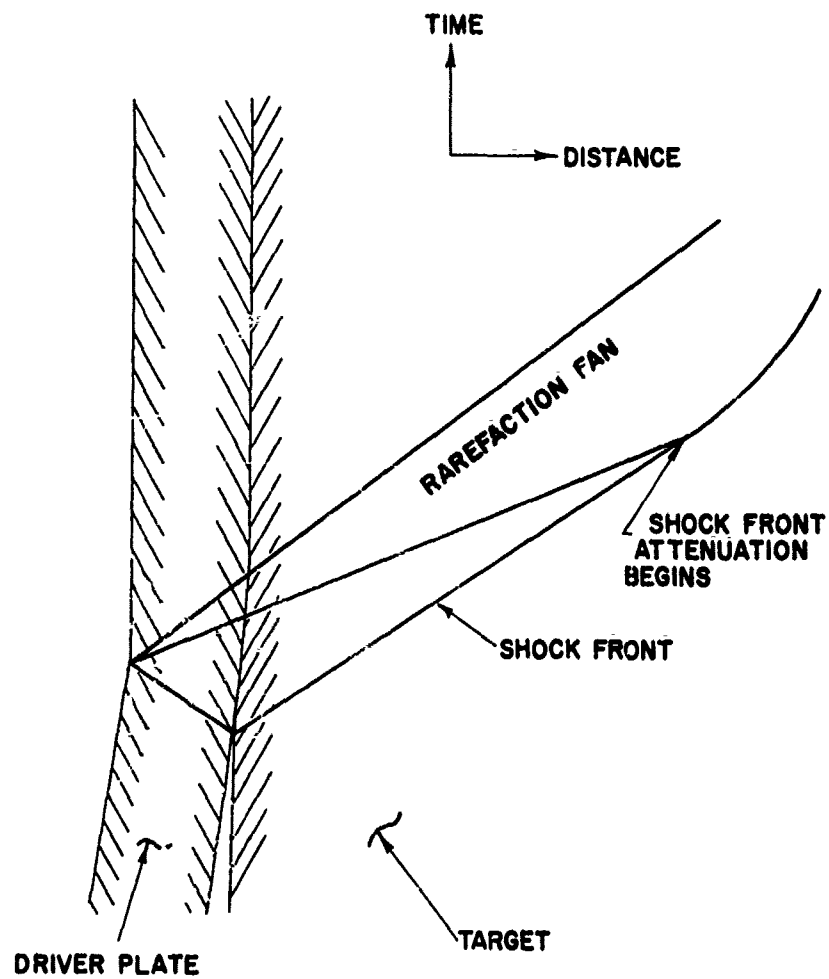


Figure 3-7. Wave Diagram for Plate Impact (Hydrodynamic Model).

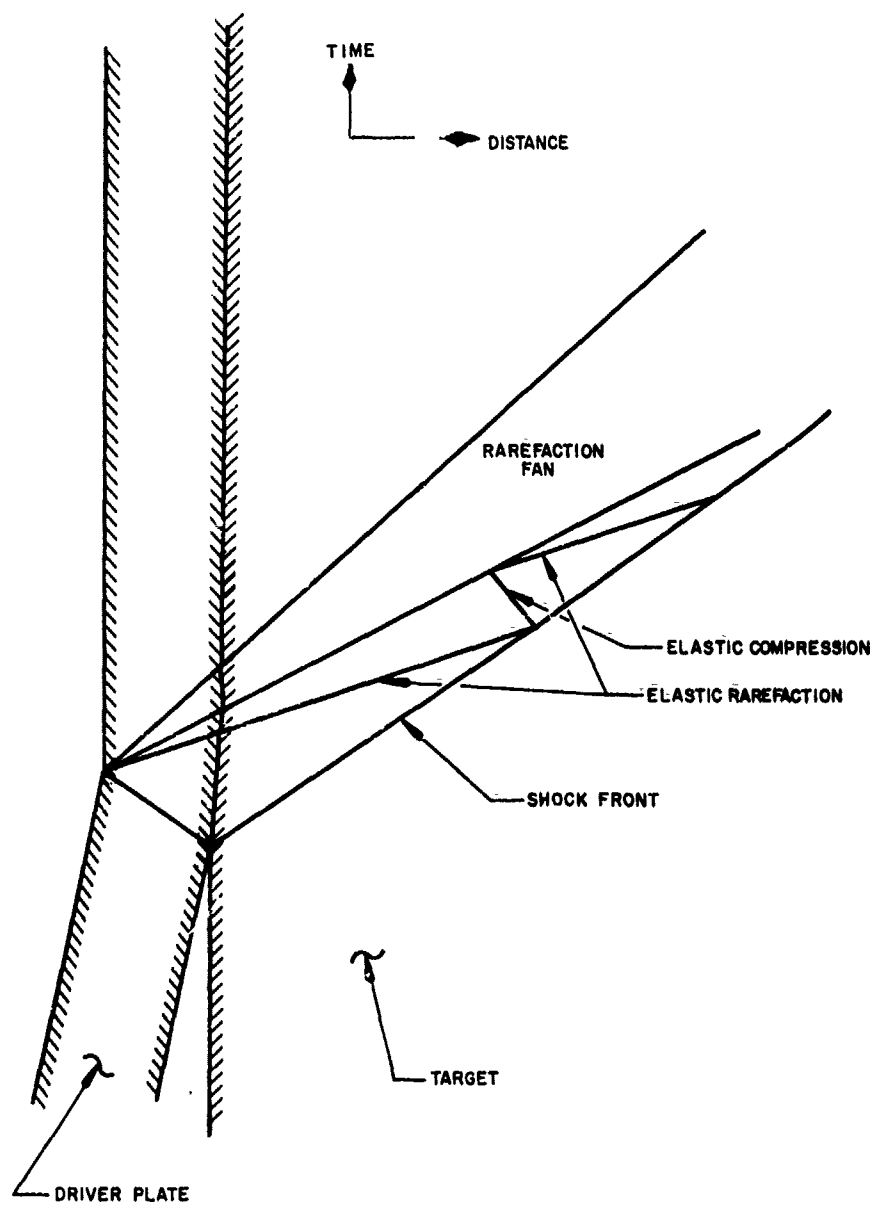


Figure 3-8. Wave Diagram for Plate Impact (Elastic-Plastic Model).

Methods of Shock-Profile Measurement

There are many methods that can be employed in determining pressure profiles for a one-dimensional shock induced into a target material. Most of these techniques infer the profile in the target from measurements made at the rear surface, either through measurement of the free-surface velocity or from the reaction of a contiguous transducer. It is also possible to chart the wave during the time of passage through the target, within restricted pressure ranges, by examining the resulting strain and/or the compression (using optical means for transparent materials or X-ray techniques for those that are opaque). In general, optical methods can only be used for comparatively low pressures, while the effectiveness of X-ray determinations is dependent on having pressures high enough to provide significant density changes. The three following experimental methods were chosen for the study, using Plexiglas as the target material:

- a. An adaptation of photostress techniques for determining the shock profile at all points within the target
- b. A type of Davies bar (Reference 15)
- c. The quartz transducer described by Jones, Neilson, and Benedick (Reference 16)

The quartz transducer would only be used to provide a basis for calibrating the other two techniques; it appears to be very accurate in the required pressure range, but becomes very expensive for measuring pulse lengths longer than 1 μ sec and would interfere with measurements performed on reflected waves. The Davies bar is capable of measuring the free-surface velocity for relatively long periods of time, while not disturbing reflection of the shock. A Davies bar of a guard-ring design is shown in Figure 3-9. Preliminary tests have been performed to determine voltage-output levels, using a target plate made of aluminum in place of Plexiglas.

Experiments were also initiated to develop photostress techniques, as illustrated in Figure 3-10. The streak-camera slit was oriented perpendicular to the impact plane. Although good film records were obtained without the Polaroid sheets, the exploding-wire light source gave an insufficient light exposure when in place to discern the photostress fringes.

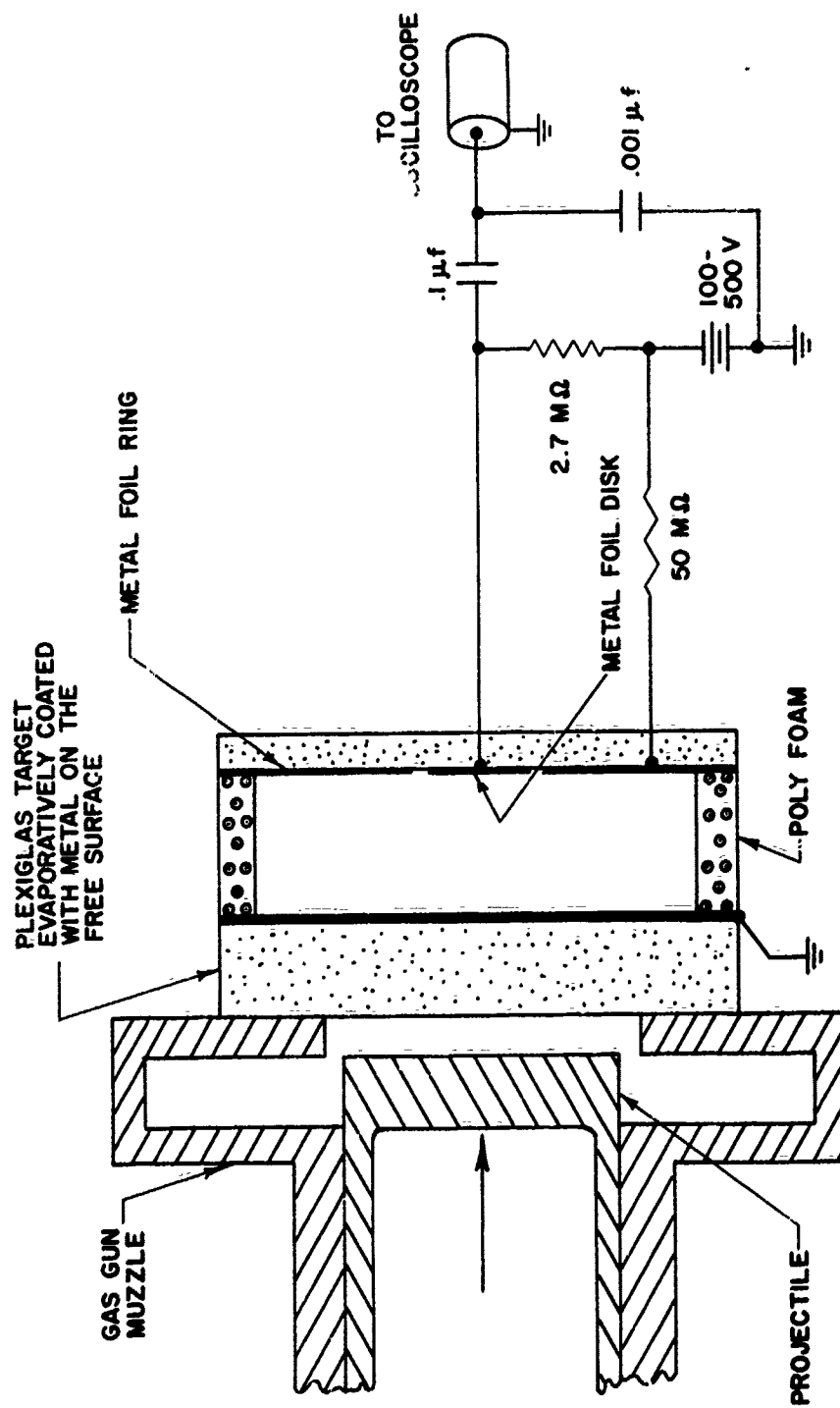


Figure 3-9. Davies Bar.

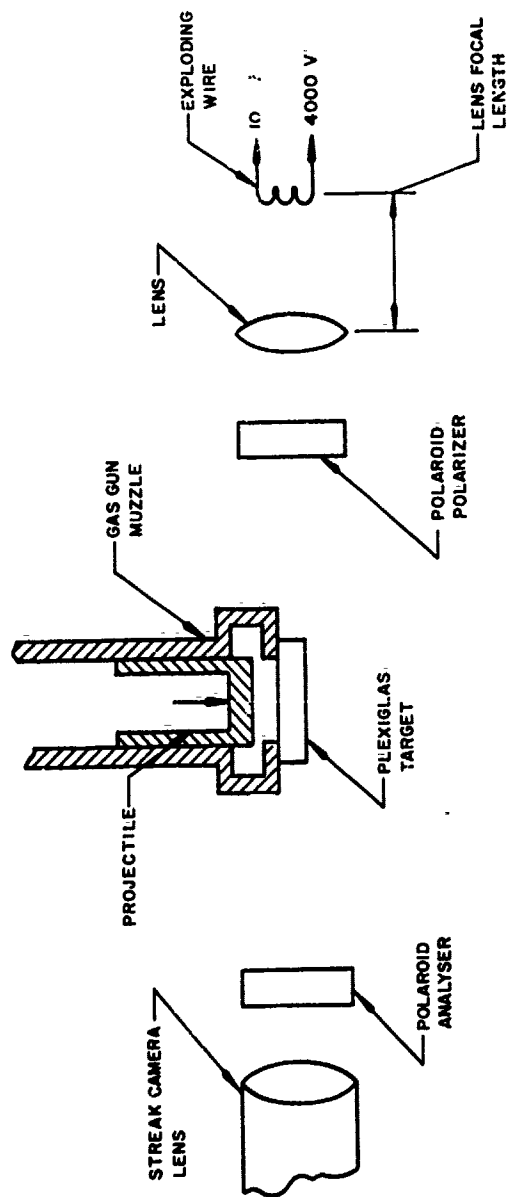


Figure 3-10. Photostress Experiment.

Time Delay of Spallation

Although it is well established at the lower tensile stress levels that the strength (fracture characteristics) of a material is a function of the loading time, there is a paucity of experimental data as to the real significance of this observation under shock-loading conditions. The preceding discussion indicates some of the complexities of obtaining meaningful data under these conditions. Zhurkov and Tomoshevskii (Reference 17) studied the fracture of Lucite under simple tension and found the fracture-delay time to vary in an inverse exponential manner with the applied stress, as most materials do. Keller and Trulio (Reference 18) recently found that the tensile stress required to spall Lucite in one-dimensional impulsive loading was about 1 kbar, which was constant over the loading duration of 2×10^{-7} to 5×10^{-6} sec. These investigators concluded that, within the accuracy of the experiments, the spall mechanism is independent of time. However, it is to be emphasized (as noted by Keller and Trulio) that the expression Zhurkov found to describe the fracture time is an extremely sensitive function of stress, and within the loading time used in the experiments the change in fracture stress required is of the same order as the experimental error in stress. Thus, a much larger range of loading times (or a different experimental technique) seems necessary to adequately measure the fracture-delay time of materials under shock-loading times.

4. EQUATION-OF-STATE MEASUREMENTS

Hugoniot equation-of-state measurements were made for four re-entry materials (chopped nylon phenolic, Series 124A resin, RAD 60, and Avcoat II), using the deceleration method described in References 4 and 19. In this technique, the dynamic-compression values are obtained by measuring both the impact velocity of a driver plate on the test sample and the wave velocity of the resultant shock. By employing a gas gun, made available from another program, and the explosive configurations previously developed under Contract AF29(601)-1760 (Reference 4), a possible induced-shock pressure range was obtained from sub-kilobar values to above 100 kilobars.

a. DETERMINATION OF SHOCK-WAVE VELOCITY

Shock waves passing through the test samples were detected using ceramic transducers (0.25-in.-dia x 0.10-in.-thick Clevite Type-4100-5 PZT disks, coated on the flat faces with silver). The faces

were designated such that when a compressive wave was propagated into the driver-electrode face, a positive signal was developed at the opposite face (the output electrode). Tests were performed using a small ram assembly, as shown in Figure 4-1.

Sheets of the test material were cut up to yield as many 4-in.-sq test blocks as possible. The faces of the blocks were milled just enough to make them smooth and parallel; two 0.313-in.-dia flat-bottom holes were drilled in one face of the block to between 0.075 and 0.100 in. from the other face. A 0.250-in. disk of 2-mil gold foil with a 1-in.-long tab was attached to the driver electrode of a transducer and cemented to the bottom of each hole with epoxy resin under pressure. As shown in Figure 4-2, two transducers were attached in the preceding manner to the surface of the block (on the same side and perpendicular to the line of hole centers).

To prepare several test blocks concurrently and to ensure adequate pressure and accurate placement of the transducers, jigs were fabricated and employed as illustrated in Figure 4-3. After bonding was completed, the distance of the output electrode from the undrilled face of the target was measured to within 0.0005 in. By subtracting from this reading the value of the thickness of the transducer, also measured to 0.0005 in., the distance of the driver electrode from the undrilled face (subsequently the impact face of the target) was known to within 0.001 in. The center conductor of a coaxial cable was connected to the output electrode of each of the transducers, and the tabs of the gold discs were electrically connected together to serve as the common ground for the shields of the coaxial lines. The transducers were then potted with epoxy, as shown in Figure 4-4.

Data-Recording Techniques

When the shock front passed through the driver electrode, positive signals were developed on the output electrode. These signals were distributed through the coaxial cables to two rasteroscilloscopes (Figure 4-5), each of which employed two display tubes: the master and slave units. Timing markers were simultaneously fed to both units.

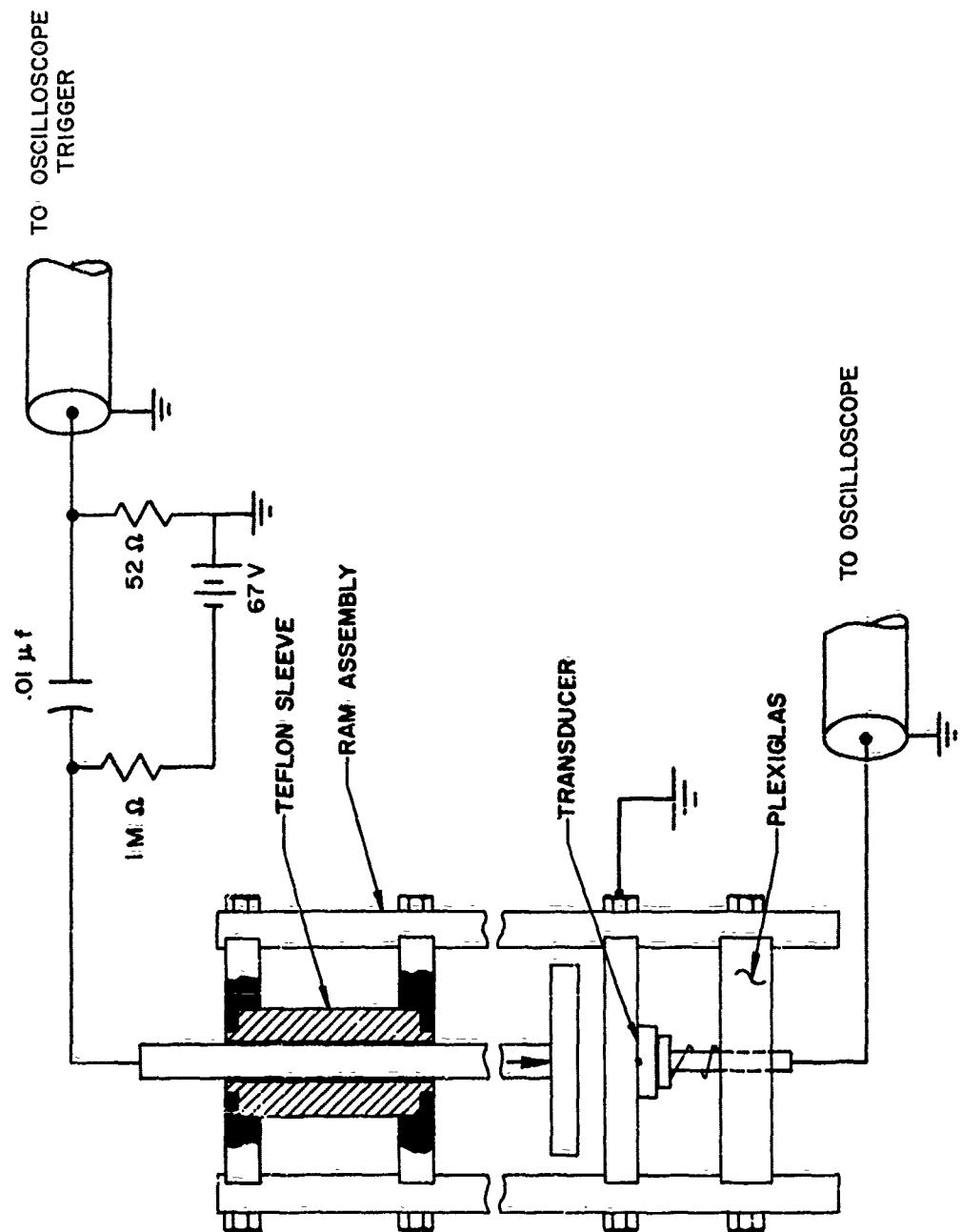


Figure 4-1. Transducer Polarity Tester.

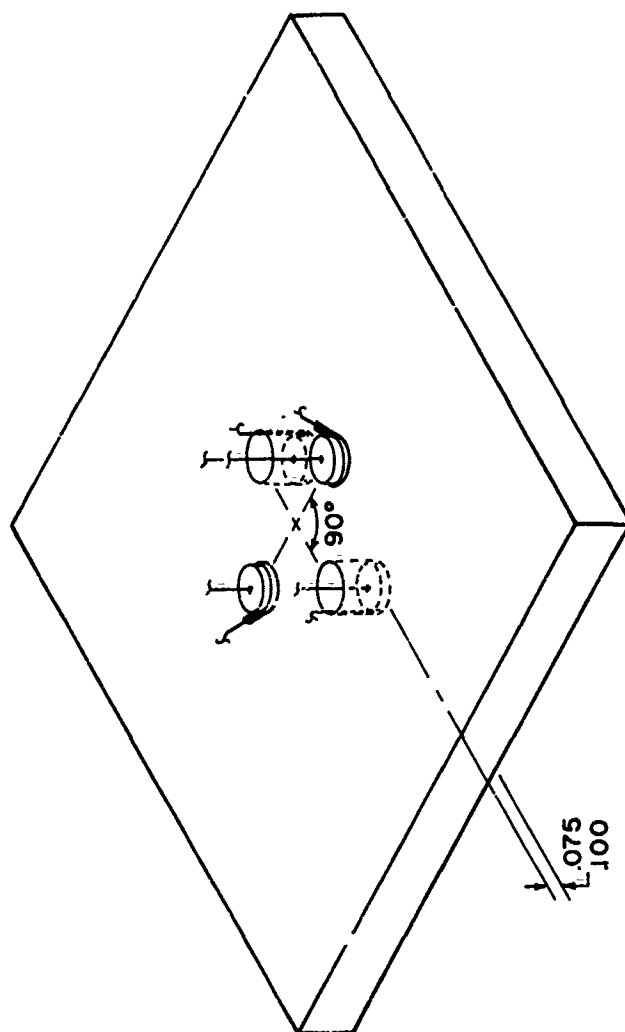


Figure 4-2. Transducer Placement.

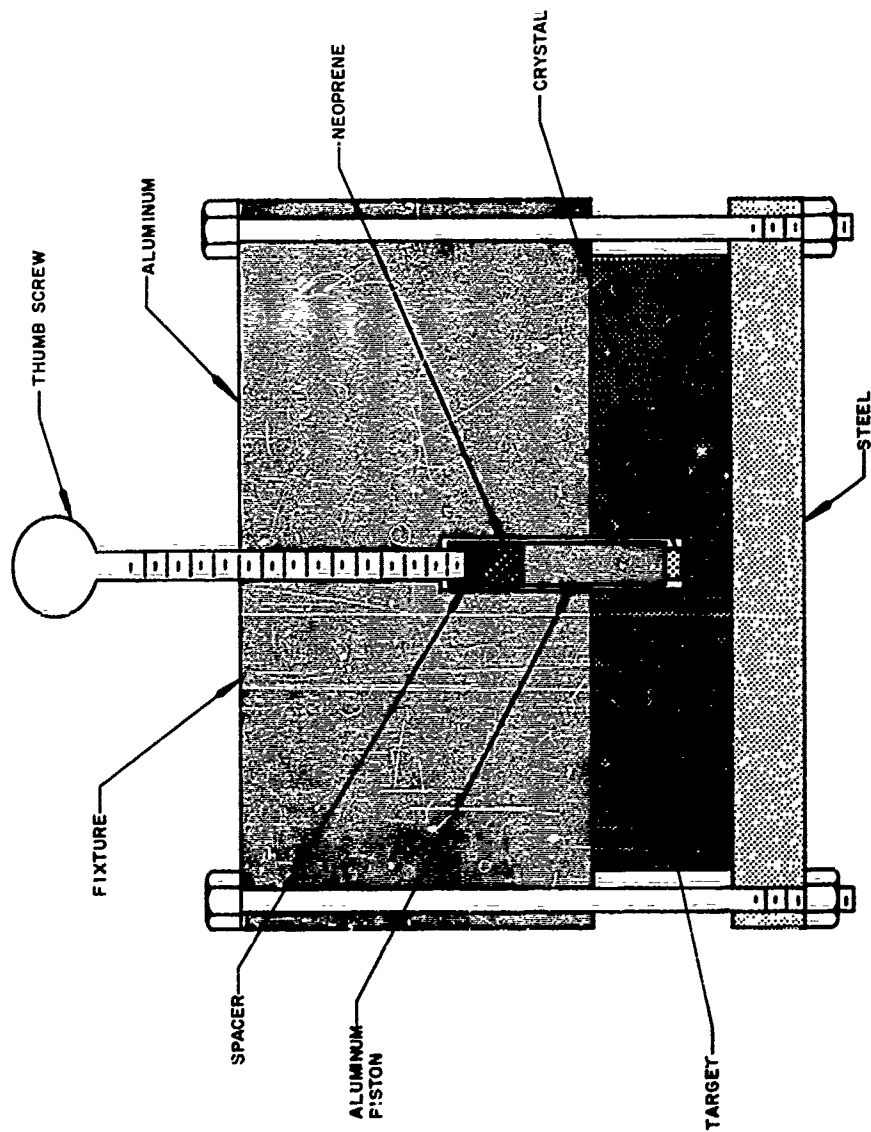


Figure 4-3. Transducer Jig.

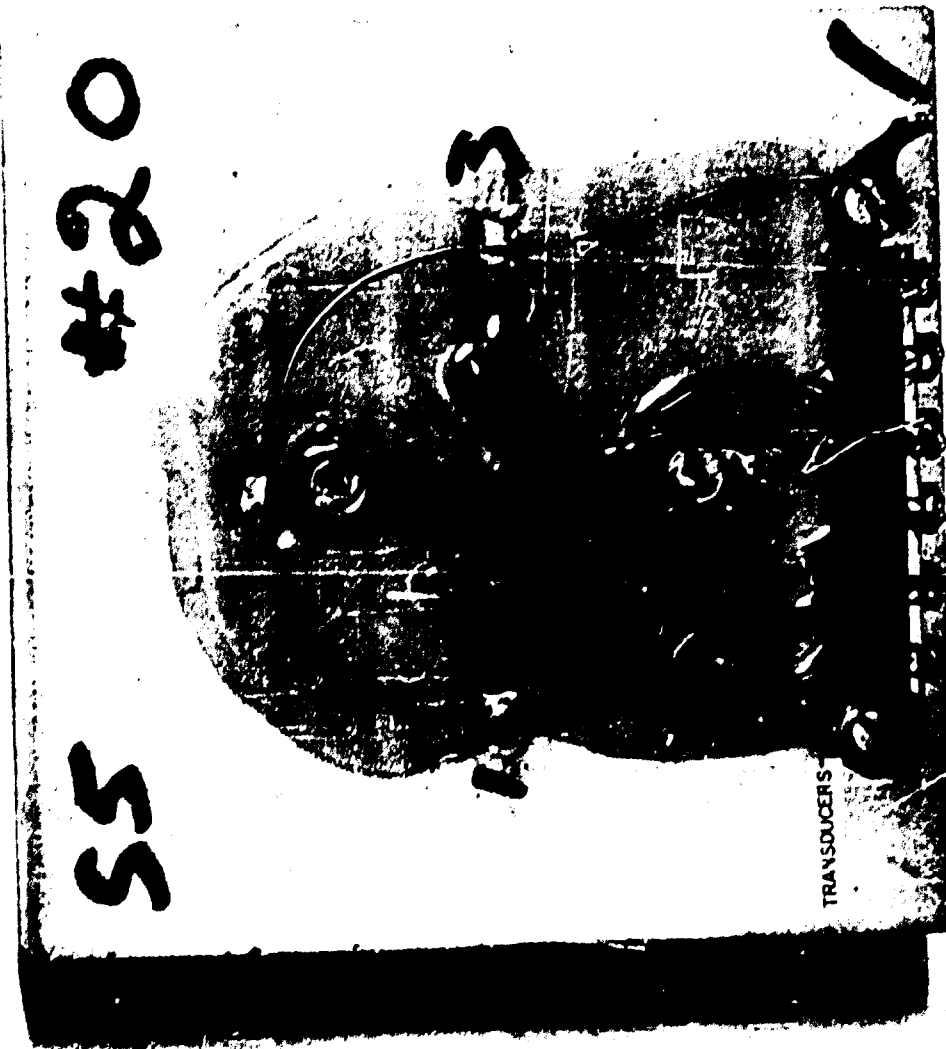


Figure 4-4. Target With Transducer Assembly.

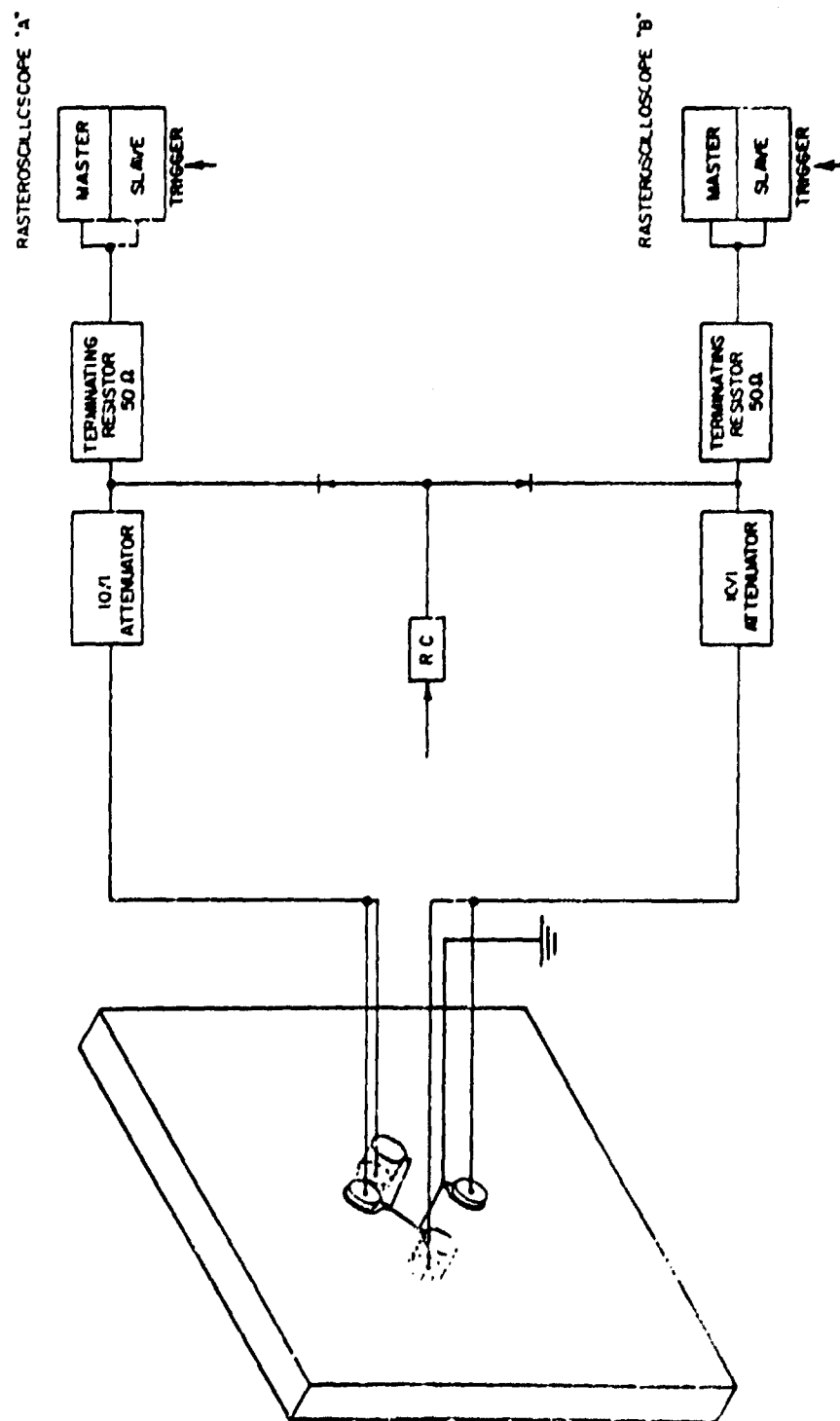


Figure 4-5. Test Circuit.

The sweep of the slave unit was slightly delayed with respect to that of the master, so that signals occurring during the retrace on one tube appeared on the other. To avoid confusion resulting from the appearance of two signal pulses at the same time, only two signals (one from each of the sets of transducers at the two distances from the impact surface) were sent to each raster oscilloscope. The two sets of data were fixed with respect to each other in time by simultaneously sending an R-C discharge timing signal to both raster oscilloscopes between the time of triggering and the appearance of the first signal. Diodes were incorporated into the timing-signal circuit to avoid interference between the two sets of transducer signals. A typical film record is presented in Figure 4-6.

Data-Reduction Method

Using an optical comparator, film records of the raster oscilloscope displays were analyzed in the following manner to obtain the time of shock arrival at each of the transducers:

Let X_{1i} , X_{2i} , X_{3i} , and X_{4i} be the distance (in inches) of the transducers from the impact surface, in the order of increasing distance, for the i th test of a total of N tests; let T_{1i} , T_{2i} , T_{3i} , and T_{4i} be the times (in microseconds), measured from a convenient time base, respectively corresponding to the shock arrival at X_{1i} , X_{2i} , X_{3i} , and X_{4i} . If a is the distance in a line parallel to the impact face between the centers of the transducers at X_1 and X_2 and c is the corresponding distance for the transducers at X_3 and X_4 , then the component of the velocity of the shock in a direction perpendicular to the impact face, V_i , is

$$V_i = \frac{(Y_{1i} + Y_{2i}) - (X_{1i} + X_{2i})}{(T_{3i} + T_{4i}) - (T_{1i} + T_{2i})} \text{ in}/\mu\text{sec} \quad (4-1)$$

The angle of tilt of the shock front with respect to the a axis is then

$$\phi_{1i} = \tan^{-1} \left| \frac{V_i (T_{2i} - T_{1i}) - (X_{2i} - X_{1i})}{a_i} \right| \quad (4-2)$$

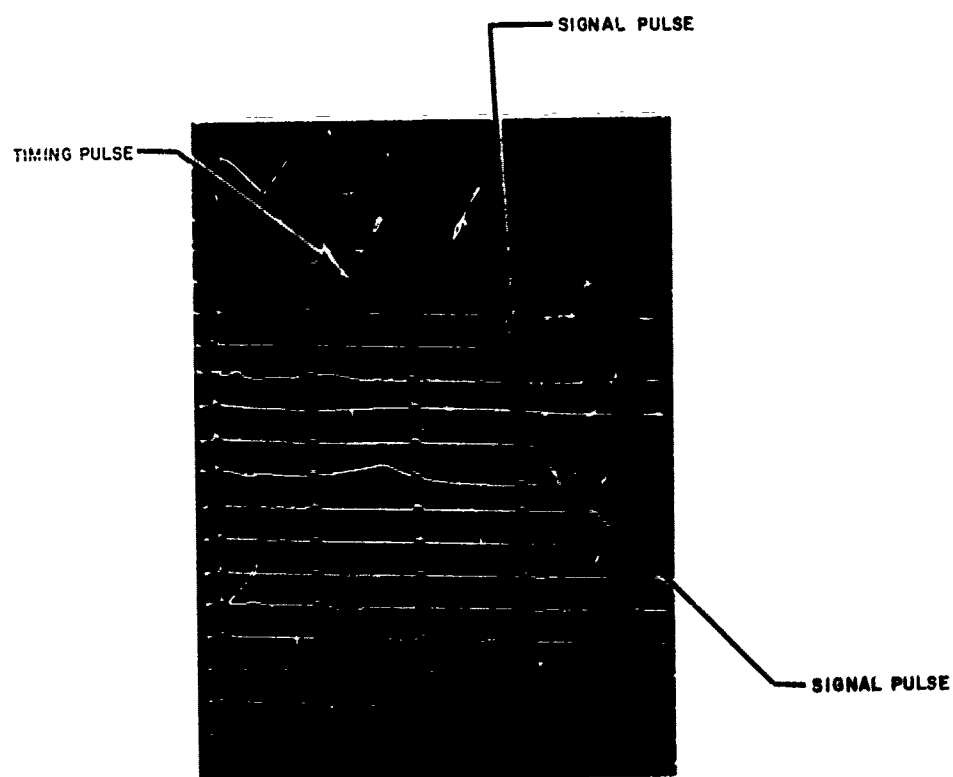


Figure 4-6. Typical Film Record.

and the angle of tilt with respect to the \underline{c} axis is

$$\phi_{2i} = \tan^{-1} \left| \frac{V_i (T_{4i} - T_{3i}) - (Y_{2i} - Y_{1i})}{c_i} \right| \quad (4-3)$$

The velocity of the shock front is

$$D_i = \frac{V_i}{\cos \phi_{1i} \cos \phi_{2i}} \cdot (25.4) \text{ mm}/\mu\text{sec} \quad (4-4)$$

and the average shock velocity is

$$\bar{D} = \frac{1}{N} \sum_{i=1}^N D_i \cdot (25.4) \text{ mm}/\mu\text{sec} \quad (4-5)$$

To determine the pressure, P , and the particle velocity, u , it is necessary to simultaneously solve (1) the wave-line equation for the test material of initial density ρ_0 ,

$$P = 10 \rho_0 D u \text{ kbar} \quad (4-6)$$

and (2) the deceleration adiabat of the driver-plate material, in this case 2024-T3 aluminum. An applicable equation was obtained by regression analysis of the combined published data from References 20 and 21.

The deceleration adiabat equation is linear up to the elastic limit of 5.82 kbar

$$P = 179.5 (W-u) \text{ kbar}; P \leq 5.82 \text{ kbar} \quad (4-7)$$

where W is the average driver-plate velocity of impact in $\text{mm}/\mu\text{sec}$.

Above 5.82 kbar, a quadratic equation was fitted to the data

$$P = 0.993 + 147.6 (W-u) + 38.45 (W-u)^2 \text{ kbar} \quad (4-8)$$

The computed value of the partic. velocity was then used to compute the dynamic compression, ρ/ρ_0

$$\rho/\rho_0 = \frac{D}{D-u} \quad (4-9)$$

A measure of the experimental precision was obtained by computing the standard deviation for the shock, S_D , and particle velocities, S_u , the pressure, S_P , and the compression, S_{ρ/ρ_0} :

$$S_D = \left[\frac{1}{N-1} \sum_{i=1}^N (D_i - \bar{D})^2 \right]^{\frac{1}{2}} \text{ mm}/\mu \text{ sec} \quad (4-10)$$

For $P \leq 5.82 \text{ kbar}$

$$S_u = \frac{\bar{u}}{\bar{W}} \left[S_W^2 + \frac{\bar{u}^2 \rho_0^2}{(179.5)^2} S_D^2 \right]^{\frac{1}{2}} \text{ mm}/\mu \text{ sec} \quad (4-11)$$

where the bars denote average values, and

$$S_W = \frac{1}{N-1} \left[\sum_{i=1}^N (W_i - \bar{W})^2 \right]^{\frac{1}{2}} \text{ mm}/\mu \text{ sec} \quad (4-12)$$

For $P > 5.82$ kbar

$$S_u = \left\{ \frac{\rho_o^2 \bar{u}^2 S_D^2 + [147.6 + 76.9 (\bar{W} + \bar{u})]^2 S_W^2}{(76.9 \bar{W} + 147.6 + \rho_o \bar{D})^2 - 153.8 (0.993 + 147.6 \bar{W} + 38.45 \bar{W}^2)} \right\}^{\frac{1}{2}}$$

mm/ μ sec (4-13)

The appropriate S_u is then used to compute S_P and $S \rho / \rho_o$ from

$$S_P = \bar{P} \left[\left(\frac{S_u}{\bar{u}} \right)^2 + \left(\frac{S_D}{\bar{D}} \right)^2 \right]^{\frac{1}{2}} \text{ kbar} \quad (4-14)$$

$$S \rho / \rho_o = \left[\frac{\bar{u}^2}{(\bar{D} - \bar{u})^4} S_D^2 + \frac{\bar{D}^2}{(\bar{D} - \bar{u})^4} S_u^2 \right]^{\frac{1}{2}} \text{ kbar} \quad (4-15)$$

An equation of state may be computed to fit the dynamic-compression data by assuming a linear relation between the shock and particle velocities, i.e., using \underline{a} and \underline{b} as constants

$$D = aU + b \text{ mm}/\mu\text{sec} \quad (4-16)$$

Equation 4-16 and the Rankine Hugoniot equations for conservation of mass and momentum can be used to derive an equation for pressure as a function of compression:

$$P = \left(\frac{b}{a-1} \right)^2 \frac{10 \rho_o (\eta - 1) \eta}{\left[\left(\frac{a}{a-1} \right) - \eta \right]^2} \text{ kbar} \quad (4-17)$$

where $\eta = \rho / \rho_o$ and the constants \underline{a} and \underline{b} are determined from Equation 4-16 by a regression analysis of the data.

b. GAS-GUN EXPERIMENTS

A 2.5-in.-dia-bore gas gun (Figure 4-7) of a design furnished by Sandia Corporation was utilized to obtain equation-of-state data in the 5- to 15-kbar range. In these tests, the shock wave was induced in the test block (placed against the muzzle of the gun) by the impact of a cylindrical bullet, which was closely fitted in the barrel and propelled from behind by high-pressure bottled-nitrogen gas let into the breech. The bullet, the barrel, and the muzzle target support were machined and aligned so that planarities could easily be kept to within 10 shakes across the impact area.

The impact velocity was determined by three small, successive, shorting pins (located near the muzzle), which projected into the barrel just enough to make electrical contact with the front edge of the bullet as it passed by. The rasteroscilloscopes were triggered by a shorting pin that projected 0.250 in. from the impact face of the test sample; the timing pulse was similarly derived from a shorting pin that projected 0.125 in. from the target (Figure 4-8). Two data points at the lower end of the desired pressure range were obtained for three materials: chopped nylon phenolic, Series 124A resin, and Avcoat II.

c. EXPLOSIVE-FLYING-PLATE EXPERIMENTS

Flying-plate-shock inputs for test samples in the 20- to 150-kbar range were provided by 5-in.-sq x 0.125-in.-thick 2024-T3 aluminum plates, backed by the explosive configurations shown in the following:

Configuration	Explosive	Inclination Angle (°)	Plate Velocity (mm/ μ sec)
A4	DuPont EL 506 A (area density: 4 gm/in. ²)	9.5	1.19
A8	DuPont EL 506 A (area density: 8 gm/in. ²)	14.0	1.91
CB	Composition B (thickness: 0.75 in.)	21.0	3.18

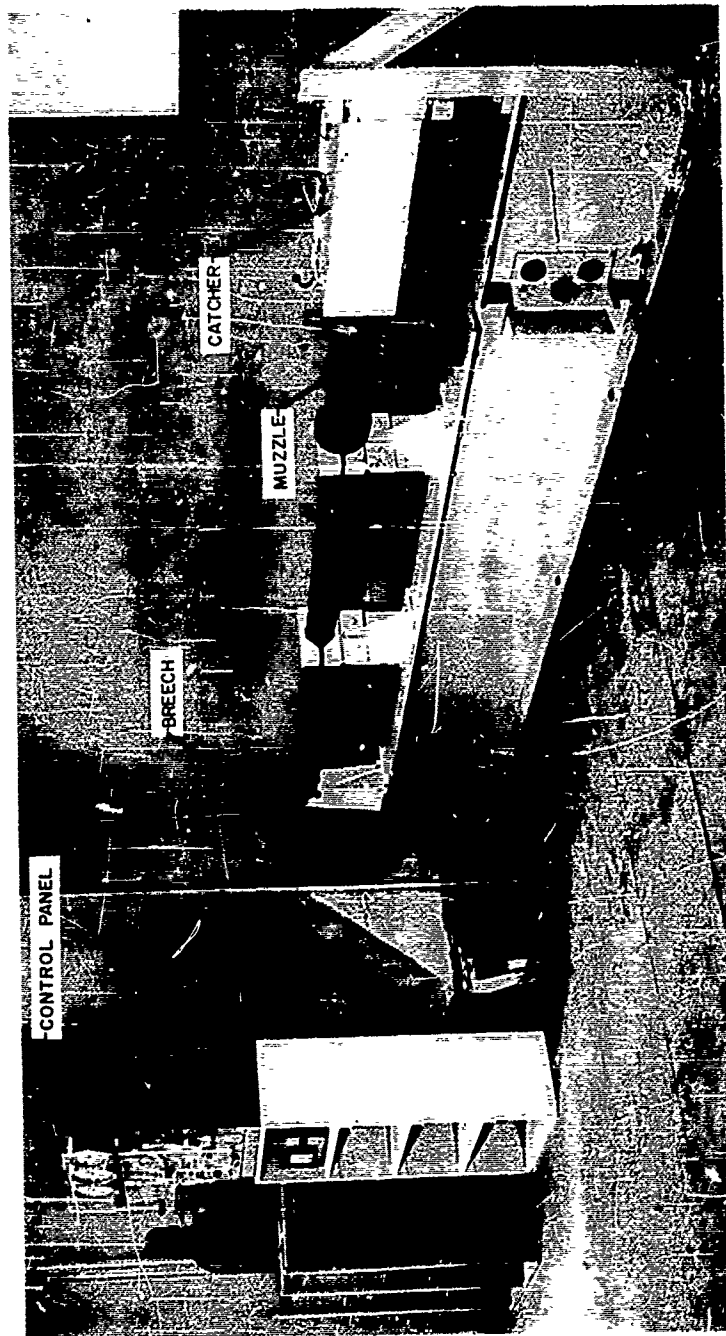


Figure 4-7. Gas Gun.

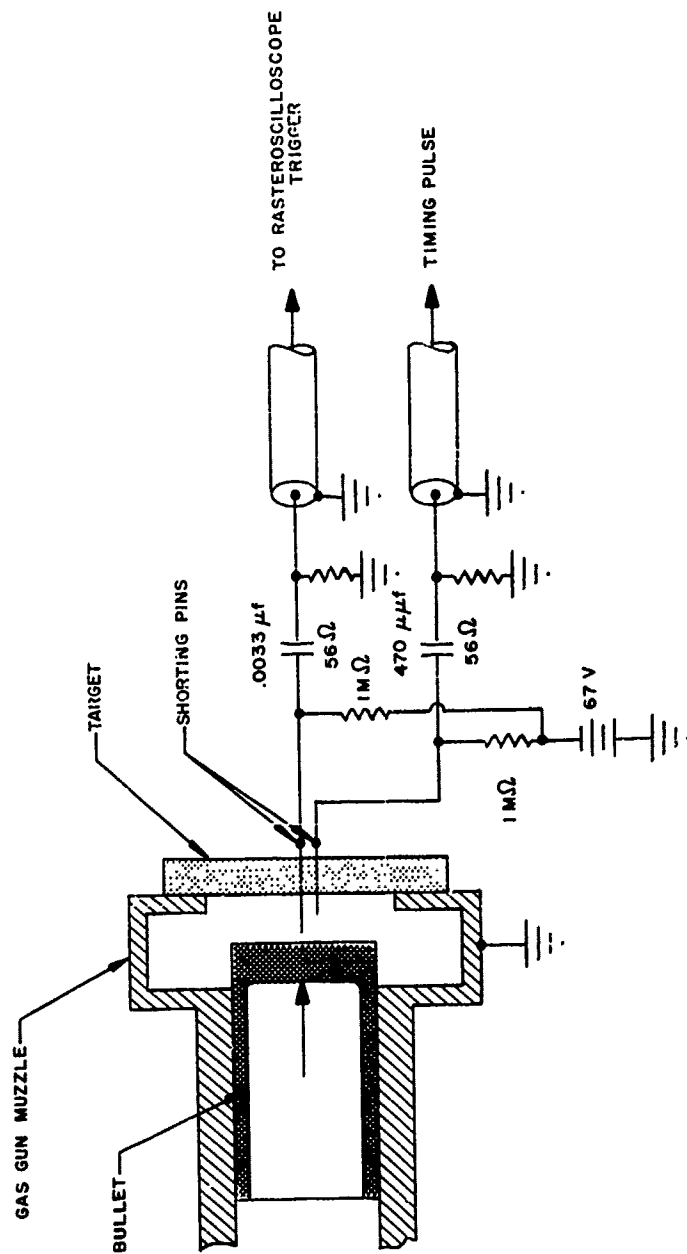


Figure 4-8. Triggering and Timing-Pulse Circuit for Gas-Gun Tests.

Rasteroscilloscope triggering was accomplished using a conduction or shorting double-probe, which was placed in the explosive train and provided an R-C pulse when passed by the detonation wave. The timing pulse was derived from the trigger pulse through a time-delay circuit (Figure 4-9).

d. EXPERIMENTAL RESULTS

Dynamic-compression data obtained in the experimental work are shown in Table 4-1. From these data, the equation of shock velocity vs particle velocity and the associated Hugoniot equation of state were computed for each material, as listed on the following page. Graphs of the equations and the experimental points are presented in Figures 4-10 through 4-17.

Avcoat II

$$(\rho_o = 1.10)$$

$$D = 1.66 u + 2.02 \text{ mm}/\mu\text{sec}$$

$$P = 103 \frac{\eta(\eta-1)}{[2.52 - \eta]^2} \text{ kbar}$$

Chopped Nylon Phenolic (CNP)

$$(\rho_o = 1.21)$$

$$D = 1.18 u + 2.95 \text{ mm}/\mu\text{sec}$$

$$P = 3250 \frac{\eta(\eta-1)}{[6.55 - \eta]^2} \text{ kbar}$$

RAD 60

$$(\rho_o = 1.30)$$

$$D = 1.07 u + 1.53 \text{ mm}/\mu\text{sec}$$

$$P = 6210 \frac{\eta(\eta-1)}{[15.3 - \eta]^2} \text{ kbar}$$

Series 124A Resin

$$(\rho_o = 1.22)$$

$$D = 1.40 u + 2.40 \text{ mm}/\mu\text{sec}$$

$$P = 439 \frac{\eta(\eta-1)}{[3.50 - \eta]^2} \text{ kbar}$$

Table 4-1. Dynamic-Compression Data.

Material	Test Configuration	Driver-Plate Impact Velocity (mm/ μ sec)		Shock Velocity (mm/ μ sec)		Particle Velocity (mm/ μ sec)		Pressure (k bar)		Compression	
		Average	Standard Deviation	Average	Standard Deviation	Average	Standard Deviation	Average	Standard Deviation	Average	Standard Deviation
Avcoat II ($\rho_0 = 1.10$)	Gas Gun	0.167	0.001	2.29	0.04	0.146	0.001	3.69	0.068	1.068	0.001
	Gas Gun	0.372	0.002	2.52	0.05	0.319	0.003	8.86	0.191	1.145	0.004
	A4	1.19	0.02	3.61	0.46	0.954	0.041	37.9	5.07	1.359	0.064
Chopped Nylon Phenolic ($\rho_0 = 1.21$)	Gas Gun	0.195	0.001	3.17	0.06	0.160	0.001	6.15	0.12	1.053	0.001
	Gas Gun	0.375	0.001	3.35	0.02	0.301	0.001	12.2	0.1	1.099	0.001
	A4	1.19	0.02	3.84	0.06	0.924	0.040	42.9	2.0	1.317	0.019
	A8	1.91	0.02	4.74	0.65	1.43	0.05	81.6	3.1	1.434	0.021
RAD 60 ($\rho_0 = 1.30$)	A8	1.91	0.02	3.17	0.21	1.53	0.05	63.0	4.8	1.930	0.136
	CB	3.18	0.11	4.14	0.31	2.44	0.40	131	23	2.433	0.623
Series 124A Resin ($\rho_0 = 1.22$)	Gas Gun	0.189	0.004	2.60	0.04	0.161	0.003	5.10	0.13	1.065	0.002
	Gas Gun	0.371	0.003	2.87	0.09	0.306	0.004	10.7	0.4	1.119	0.004
	A4	1.19	0.02	3.68	*	0.931	*	41.8	*	1.379	*
	A8	1.91	0.02	4.43	*	1.44	*	78.0	*	1.485	*

* Insufficient number of data points on which to calculate standard deviation.

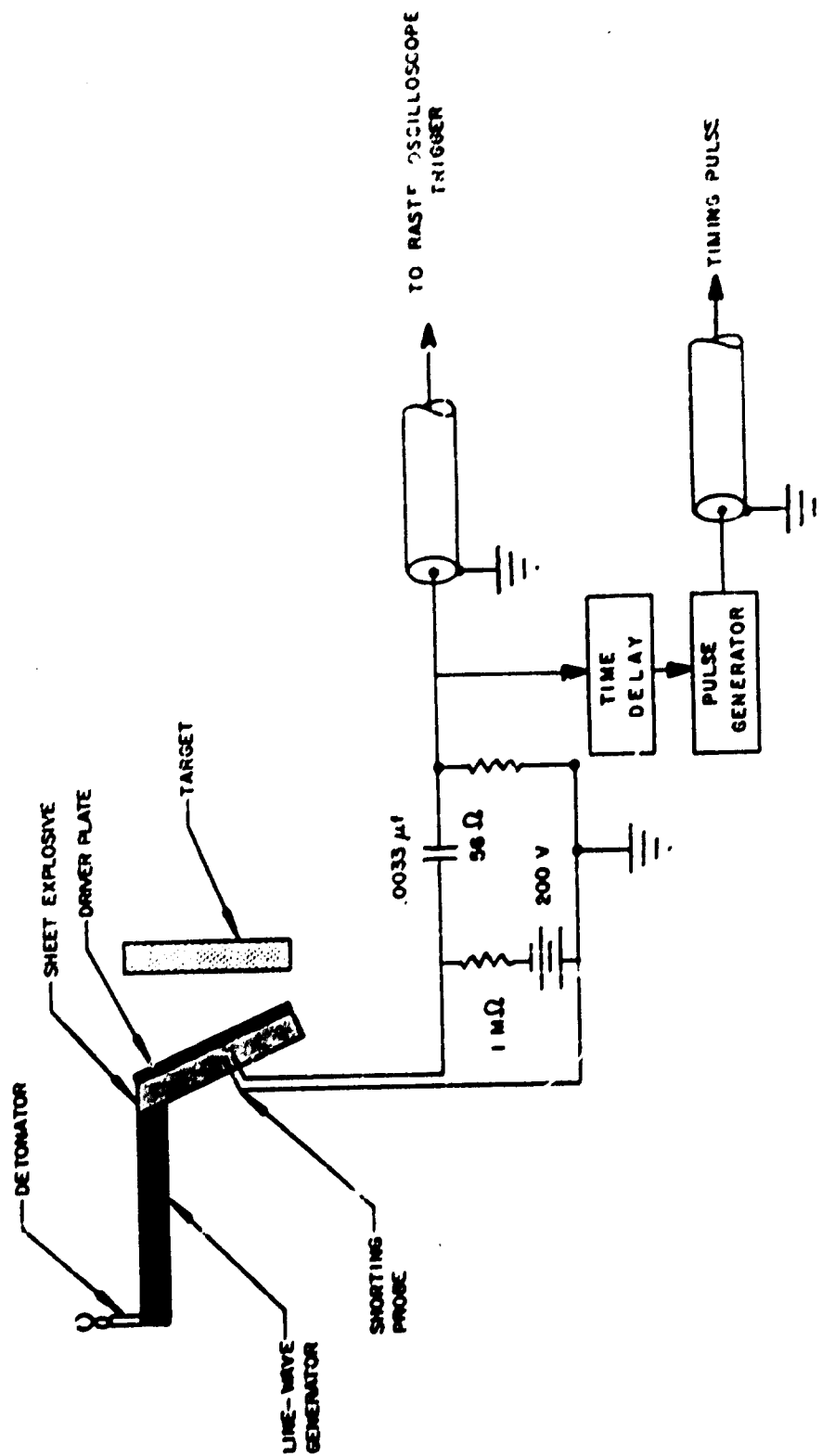


Figure 4-9. Triggering and Timing-Pulse Circuit for Explosive Tests.

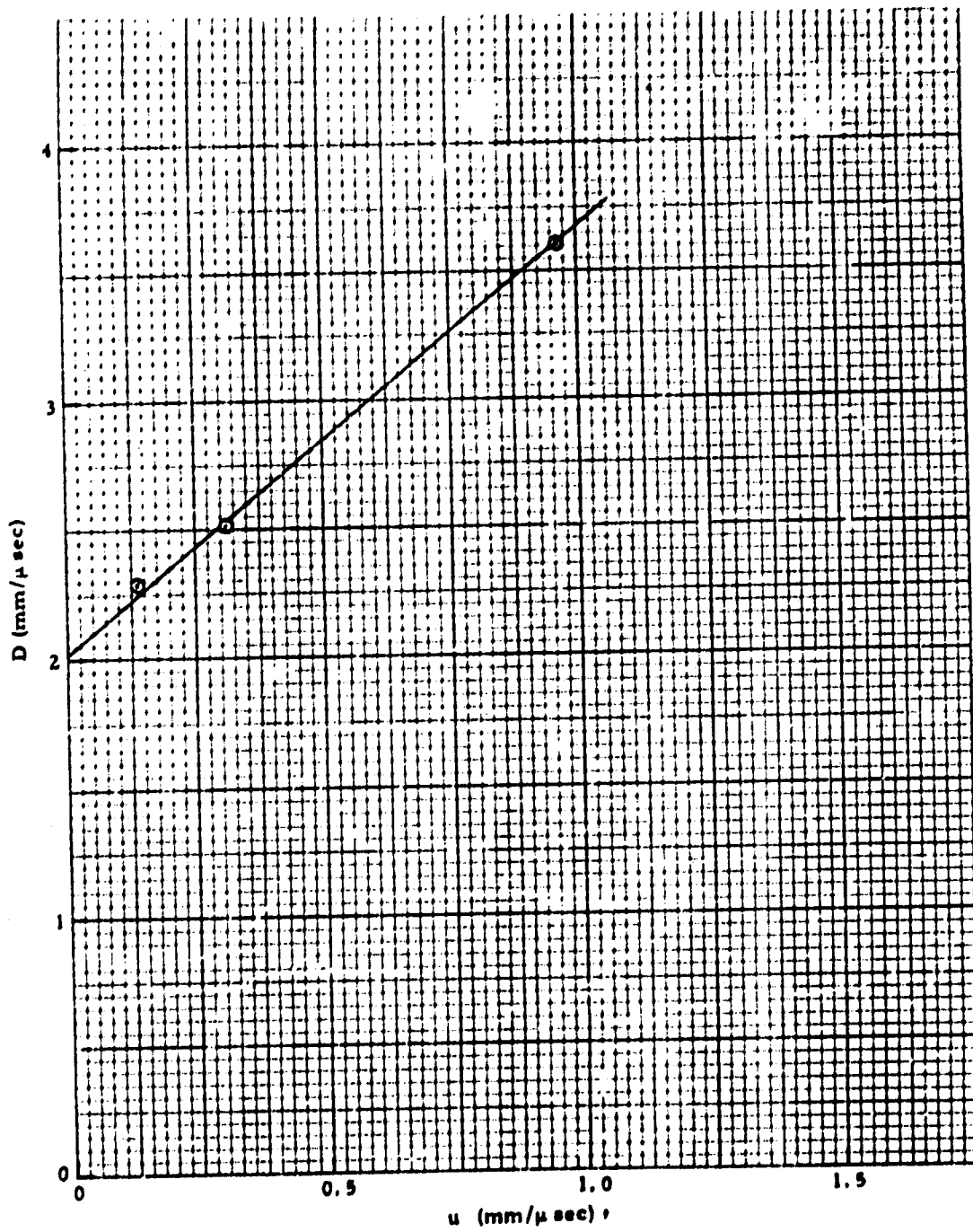


Figure 4-10. Shock Velocity vs Particle Velocity (Avcoat II).

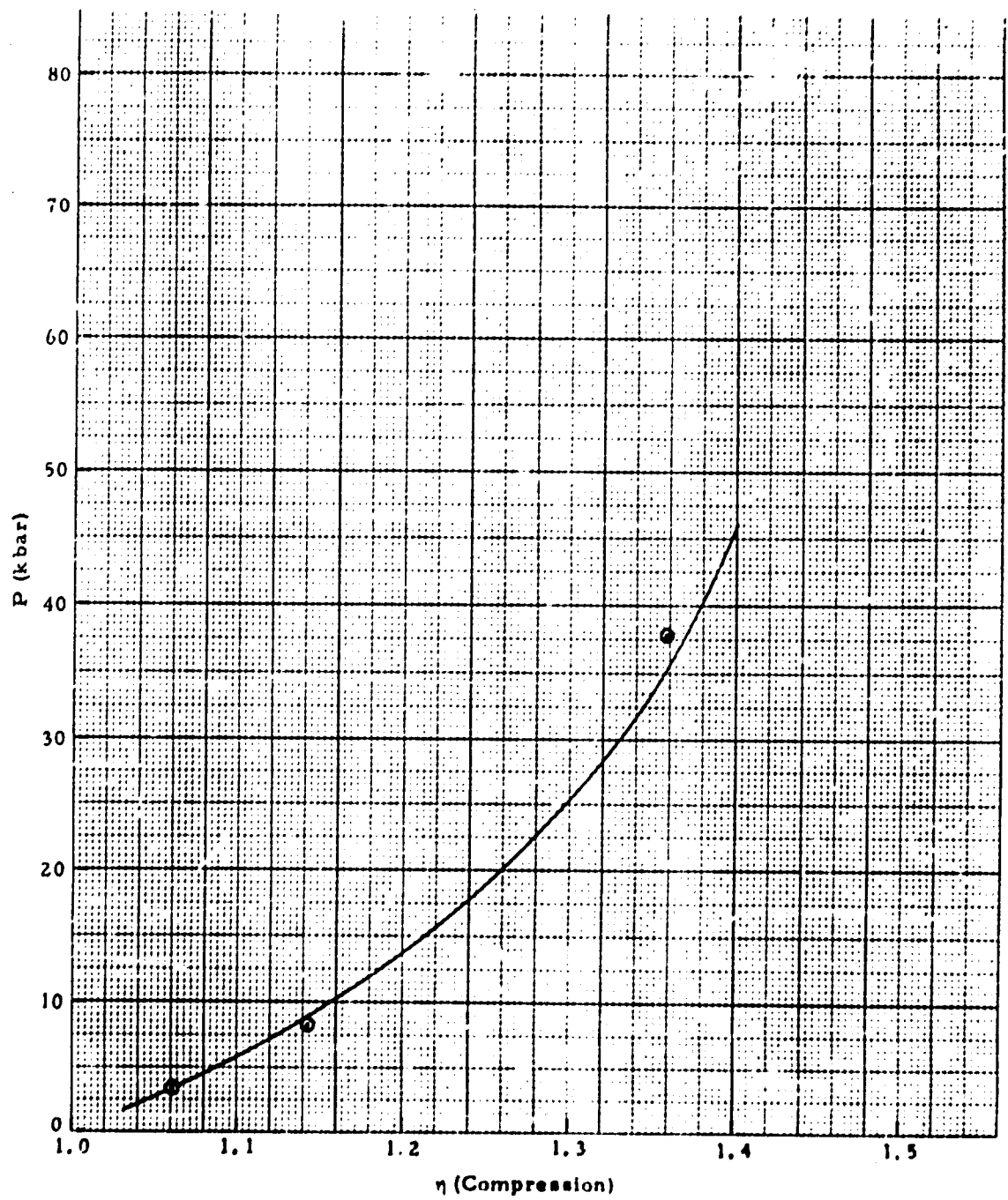


Figure 4-11. Dynamic-Compression Curve (Avcoat II).

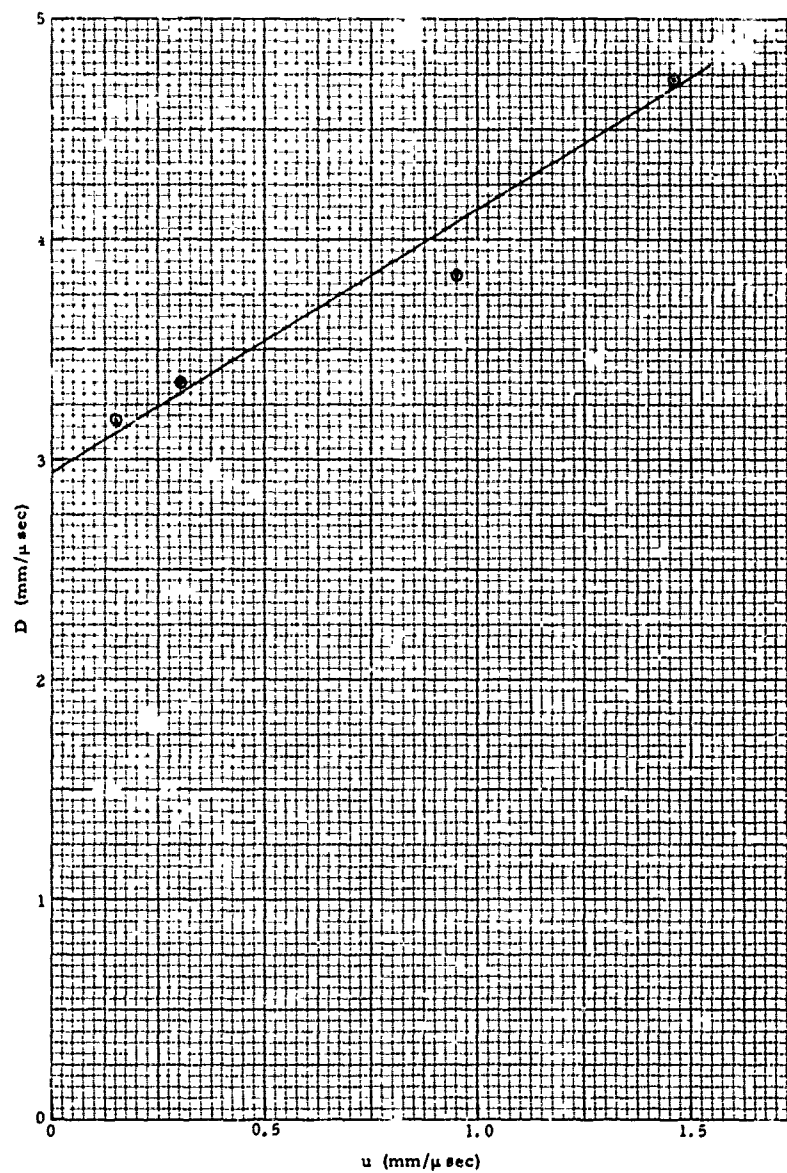


Figure 4-12. Shock Velocity vs Particle Velocity (Chopped Nylon Phenolic).

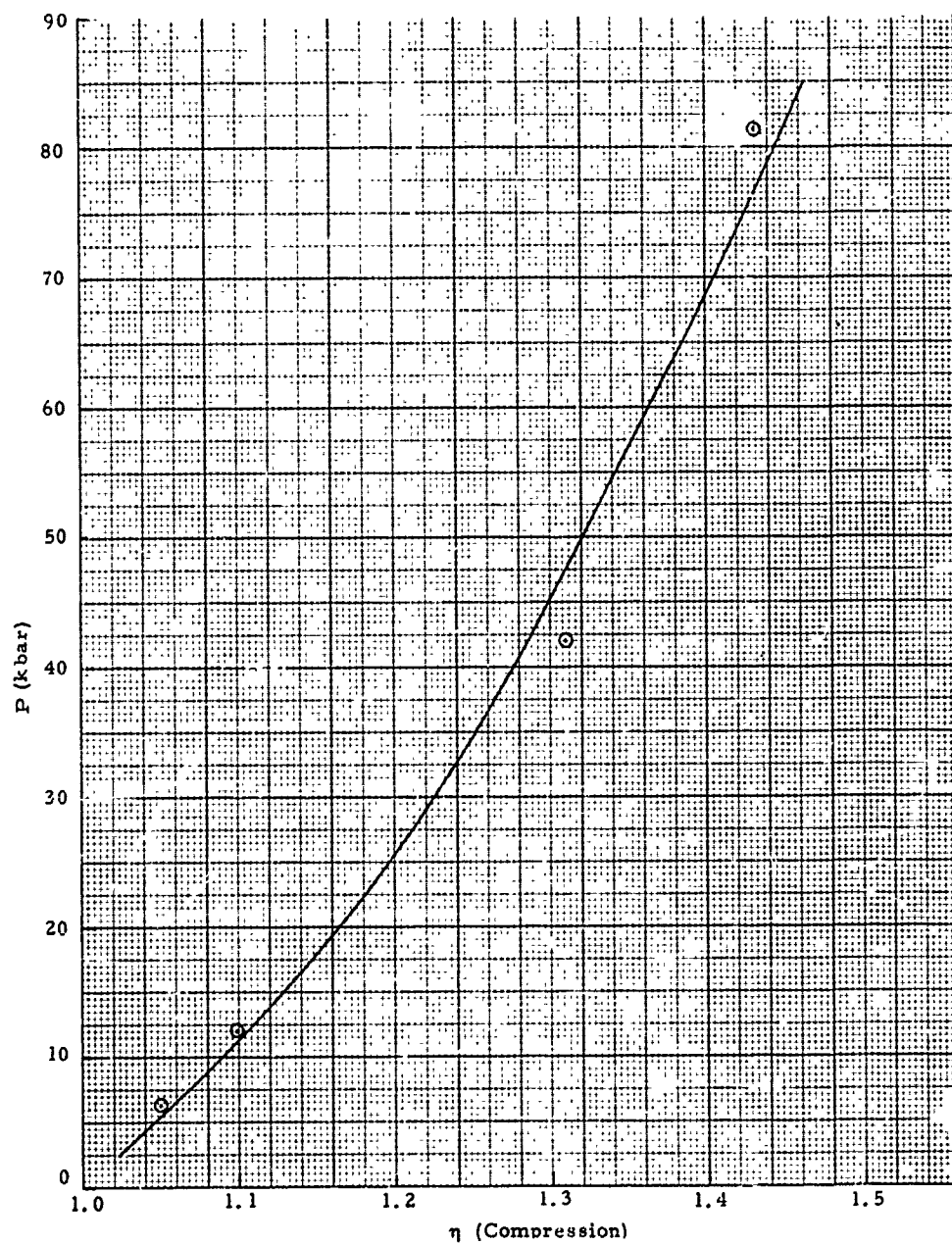


Figure 4-13. Dynamic-Compression Curve (Chopped Nylon Phenolic).

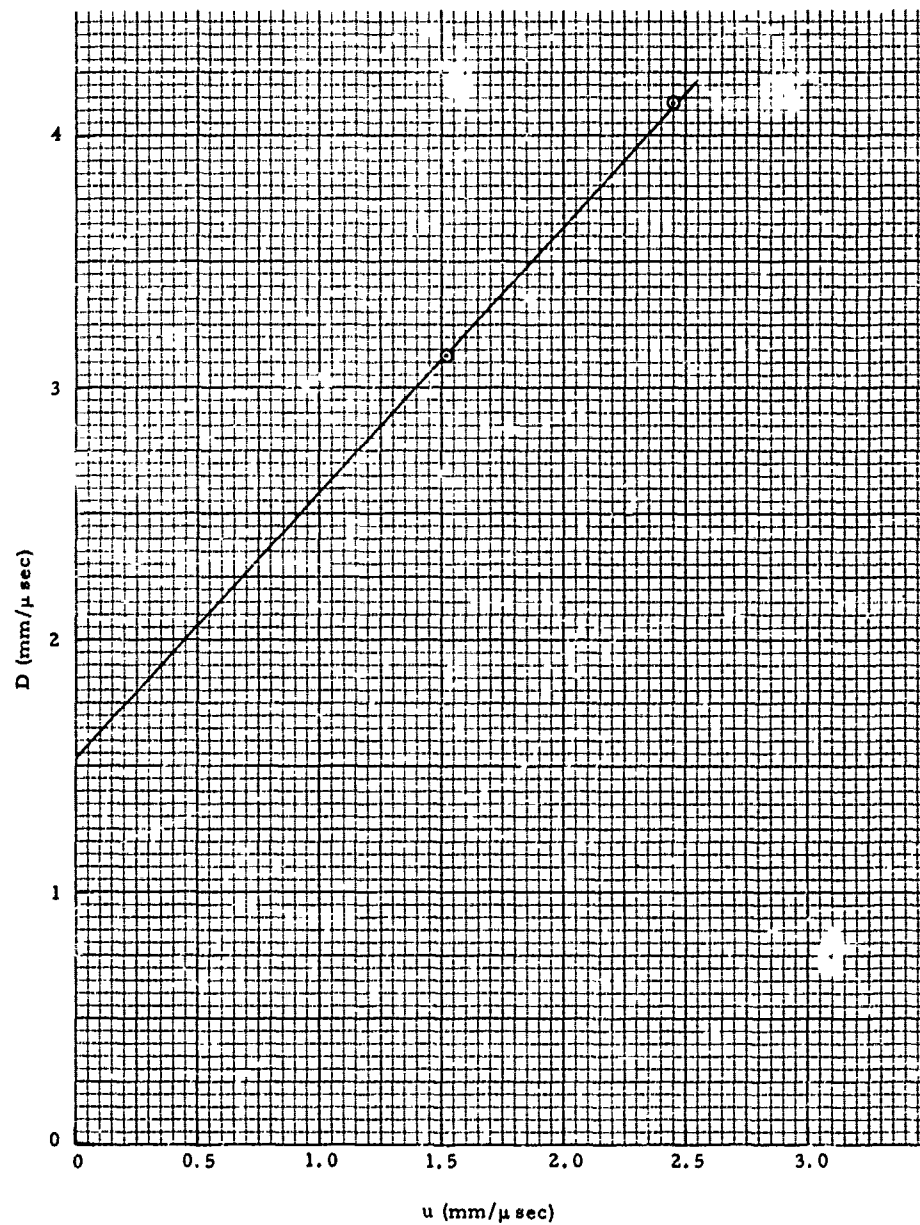


Figure 4-14. Shock Velocity vs Particle Velocity (RAD 60).

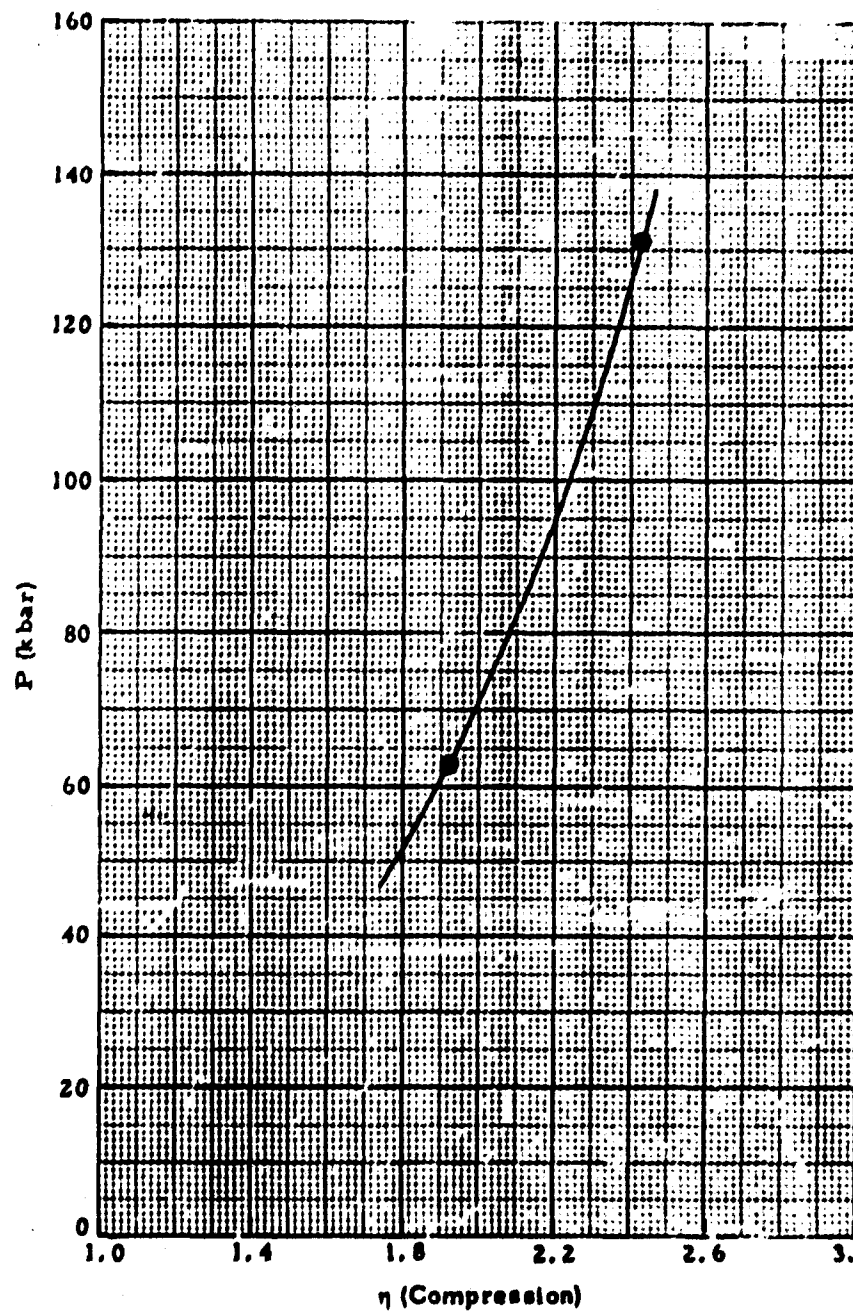


Figure 4-15. Dynamic-Compression Curve (RAD 60).

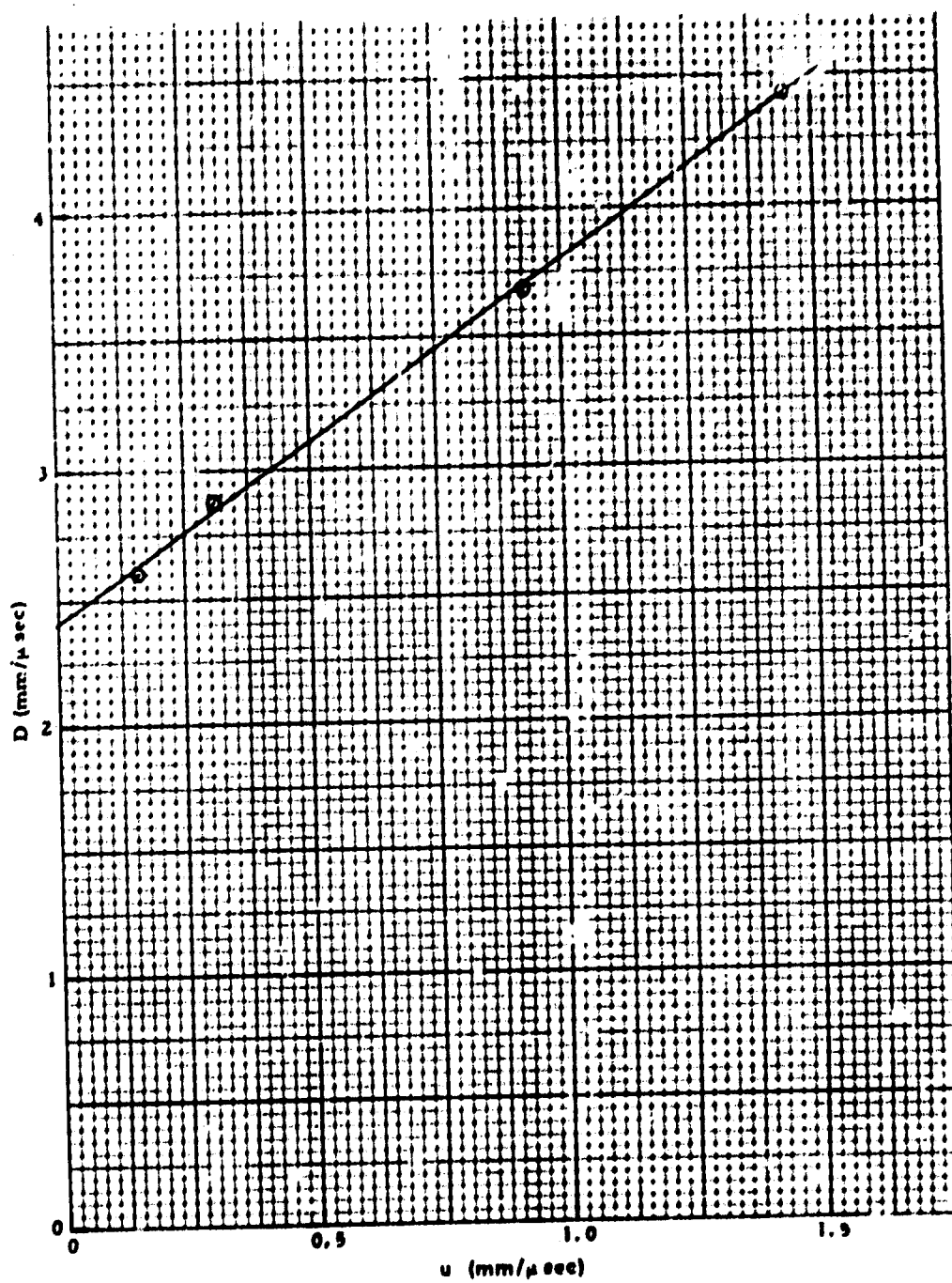


Figure 4-16. Shock Velocity vs Particle Velocity (Series 124A Resin).

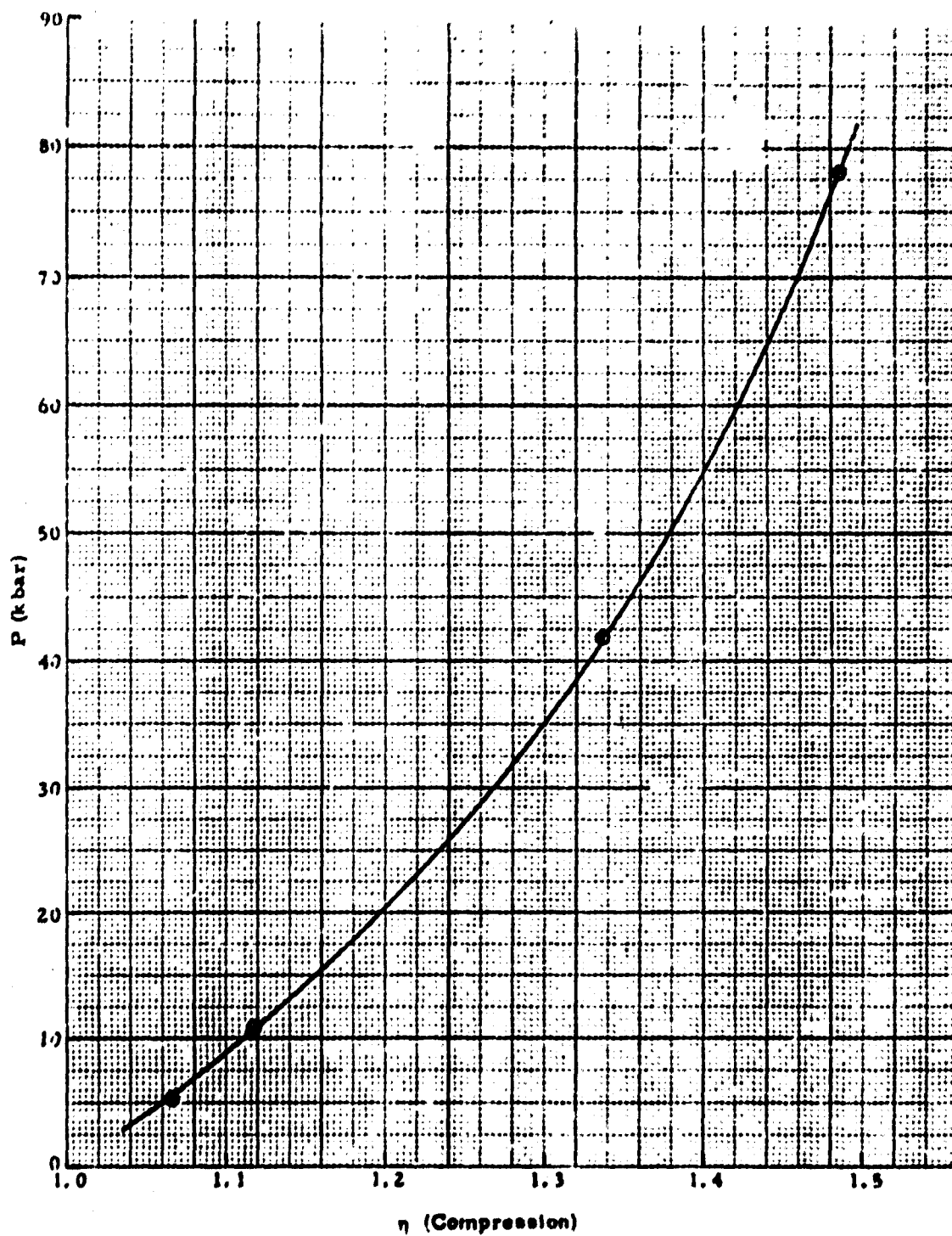


Figure 4-17. Dynamic-Compression Curve (Series 124A Resin).

REFERENCES

1. A. Tobolsky and H. Eyring, J. Chem. Phys. **11**, 125 (1943).
2. F. Bueche, J. Appl. Phys. **26**, 1133 (1955); **28**, 784 (1957); **29**, 1231 (1958).
3. S. N. Zhurkov and T. P. Sanfirova, Soviet Phys. Tech. Phys. **3**, 1586 (1958).
4. M. H. Wagner, W. F. Waldorf, and N. A. Louie, "Determination of Hugoniot Equations-of-State for Polymers and Re-entry Vehicle Materials and Investigations of Fracture Phenomena," AFSWC-TDR-62-66, Vol. 1, Aug. 1962.
5. G. R. Irwin, "Fracture by Progressive Crack Extension," Proc. Symp. on Structural Dynamics Under High Impulse Loading, ASD-TDR-63-140, Wright-Patterson Air Force Base, May 1963, pp. 293-321.
6. W. H. Andersen, "Kinetics and Mechanism of Fracture in Solid Materials," AFSWC-TDR-62-66, Vol. 1, Aug. 1962, pp. 42-50.
7. E. N. Dulaney and W. F. Brace, J. Appl. Phys. **31**, 2233 (1960).
8. J. J. Benbow, Proc. Phys. Soc. **78**, 970 (1961).
9. G. C. Sih, AIAA Journal **1**, 492 (1963).

10. M. L. Williams, J. Appl. Mech. 24, 1 (1956).
11. J. P. Berry, J. Appl. Phys. 34, 62 (1963).
12. J. R. Penning, D. M. Young, and J. H. Prindle, "Negative Equation of State and Spall Criteria," RTD-TDR-63-3039, Air Force Weapons Laboratory, Sept. 1963.
13. G. R. Fowles, J. Appl. Phys. 31, 655 (1960).
14. D. R. Curran, J. Appl. Phys. 34, 2677 (1963).
15. R. M. Davies, Trans. Roy. Soc. (London) A240, 375 (1948).
16. O. E. Jones, F. W. Neilson, and W. B. Benedick, J. Appl. Phys. 33, 3224 (1962).
17. S. N. Zhurkov and E. E. Tomoshevskii, J. Tech. Phys. (USSR) 25, 66 (1955).
18. D. V. Keller and J. G. Trullo, J. Appl. Phys. 34, 172 (1963).
19. L. V. Al'tshuler, K. K. Krupnikov, B. N. Ledenev, V. I. Zhuchikhin, and M. I. Brazhnik, Sov. Phys. JETP 34, 606 (1958).

20. G. R. Fowles, J. Appl. Phys. 32, 1475 (1961).
21. J. M. Walsh, M. H. Rice, R. G. McQueen, and F. L. Yarger,
Phys. Rev. 108, 196 (1957).

DISTRIBUTION

No. cys.

HEADQUARTERS USAF

1 Hq USAF (AFRNE-B, Maj Lowry), Wash, DC 20330
1 Hq USAF (AFTAC), Wash, DC 20330

MAJOR AIR COMMANDS

1 AFSC (SCT), Andrews AFB, Wash, DC 20331
1 AUL, Maxwell AFB, Ala 36112
1 USAFIT (USAF Institute of Technology), Wright-Patterson AFB,
Ohio 45433
1 USAFA, United States Air Force Academy, Colo 80840

AFSC ORGANIZATIONS

2 FTD (Library), Wright-Patterson AFB, Ohio 45433
1 AF Materials Laboratory, Wright-Patterson AFB, Ohio 45433
1 ASD (ASIXRR, Tech Info Ref Br., Reports Div., Marie Koeker),
Wright-Patterson AFB, Ohio 45433
1 RTD (RTS), Bolling AFB, Wash, DC 20332

KIRTLAND AFB ORGANIZATIONS

1 AFSWC (SWEH), Kirtland AFB, NM 87117
AFWL, Kirtland AFB, NM 87117
5 (WLRP)
1 (WLAX)
10 (WLL)

OTHER AIR FORCE AGENCIES

Director, USAF Project RAND, via: Air Force Liaison Office,
The RAND Corporation, 1700 Main Street, Santa Monica, Calif
90406

1 (RAND Physics Division, ATTN: Dr. Olen Nance)
1 (RAND Library)
1 AFOAR, Bldg T-D, Wash, DC 20333
1 AFOSR, Bldg T-D, Wash, DC 20333

ARMY ACTIVITIES

1 Director, Ballistic Research Laboratories (Library for Dr. Coy
Glass), Aberdeen Proving Ground, Md 21005
1 Commanding Officer, Picatinny Arsenal, Samuel Feltman
Ammunition Laboratories, ATTN: Mr. Murray Weinstein,
Dover, NJ 07801

DISTRIBUTION (cont'd)

No. cys

NAVY ACTIVITIES

- 1 Chief of Naval Research, Department of the Navy, Wash, DC 20390
- 2 Director, Special Projects, Department of the Navy, Wash 25, DC
- 1 Commander, Naval Ordnance Laboratory, ATTN: Dr. Rudlin, White Oak, Silver Spring, Md
- 1 Office of Naval Research, Wash 25, DC

OTHER DOD ACTIVITIES

- 1 Chief, Defense Atomic Support Agency (Document Library), Wash, DC 20301
- 1 Director Advanced Research Projects Agency, Department of Defense, The Pentagon, Wash, DC 20301
- 20 Hq Defense Documentation Center for Scientific and Technical Information (DDC), Bldg 5, Cameron Sta, Alexandria, Va 22314

AEC ACTIVITIES

- 1 Sandia Corporation (Information Distribution Div.), Box 5800, Sandia Base, NM 87115
- 1 Sandia Corporation (Technical Library), P.O. Box 269, Livermore, Calif 94551
- 1 University of California Lawrence Radiation Laboratory (Technical Information Div.), P.O. Box 808, Livermore, Calif 94551
- 1 University of California Lawrence Radiation Laboratory (Technical Information Div.), Berkeley 4, Calif
- 1 Director, Los Alamos Scientific Laboratory (Helen Redman, Report Library), P.O. Box 1663, Los Alamos, NM 87554

OTHER

- 1 OTS, Department of Commerce, Wash 25, DC
- 1 General Electric Company - MSD, ATTN: Dr. F.A. Lucy, Room M9505, P.O. Box 8555, Philadelphia 1, Pa
- 1 Stanford Research Institute, ATTN: Dr. G.R. Fowles, Menlo Park, Calif 94025
- 1 AVCO Corporation, Research and Advanced Development Div., ATTN: Chief Librarian, 201 Lowell Street, Wilmington, Mass
- 1 Aerojet-General Corporation, ATTN: Mr. N. A. Louie, Downey, Calif
- 1 Official Record Copy (Lt Richard C. Brightman, WLRPX)